diagnosed with preoperative PVO and functional right univentricle. We consider that intensive management is important to adjust the pulmonary blood flow in these complex patients.

POSTOPERATIVE PVO. Univentricle or heterotaxy syndrome has been identified as a risk factor for reoperation in postoperative PV stenosis [21]. The study found that 79% of reoperations for PV stenosis occurred within 6 months of the operation. Another report of 20 patients identified that postoperative PVO occurring within 6 months of the operation was a risk factor for death [22]. Residual PVO might cause subsequent pulmonary hypertension, with even worse outcomes [23].

In our study, postoperative PVO occurred in 15 patients, and of these, there were 7 hospital deaths and 4 late deaths. Univariate analysis identified postoperative PVO as a risk factor for hospital death and late death. Of 5 patients who underwent surgical repair or PTA for postoperative PVO, 4 patients underwent the procedure within 6 months after TAPVC repair and survived the perioperative period. Therefore, postoperative PVO should be repaired as soon as possible, before the pulmonary hypertension becomes persistent.

Both patients with postoperative PVO who underwent PTA died of multiorgan dysfunction, which eventually occurred due to residual pulmonary hypertension, even though PTA relieved the PVO. Another report found that high resistance of the pulmonary vasculature, caused by postoperative PVO, was the main factor influencing death in 14 autopsies of patients diagnosed with univentricle with TAPVC [18]. We consider that the PV wall cannot be normalized immediately and that the various complications might occur due to the poor general condition of the patient, even if the PVO can be relieved.

Conventional TAPVC repair may be associated with later intimal hyperplasia localized to the anastomotic site. Improvement or modification of the primary repair technique is therefore required to prevent postoperative PVO. For example, a sutureless technique that avoids trauma to the PV wall and minimizes the risk of distortion at the anastomosis has been reported [14, 16, 23]. Postoperative PVO was found in only 1 of 13 patients with RAI after use of the sutureless technique [14]. This technique may be able to prevent postoperative PVO, although the long-term surgical outcomes are unclear.

TIMING OF TAPVC REPAIR. Univariate analysis identified previous operation and concomitant Fontan procedure were protective factors for hospital death. This may indicate that results for patients who wait for their TAPVC repair, for example until after other operations or until the time of their Fontan procedure, are satisfactory.

Fontan Takedown

In our series, there was a 9.6% Fontan takedown rate, which is a high rate for a procedure usually associated with high morbidity. In general, patients with preoperative obstructed TAPVC are high-risk candidates for the Fontan operation. However, we attempt to complete the definitive procedure even if the patient has preoperative PVO. In addition, we perform concomitant TAPVC repair

and the Fontan operation to reduce surgical time as much as possible. As a result, the rates of Fontan takedown were higher than in previous reports. All patients who required Fontan takedown had preoperative or postoperative PVO. Preoperative PVO may be associated with residual pulmonary hypertension, leading to collapse of the Fontan circulation.

Strategies to Contribute to Improvement of Surgical Outcomes

1. Improvement or modification of the primary repair technique is required to avoid postoperative PVO, such as using the sutureless technique, especially in patients with extracardiac TAPVC.
2. Postoperative PVO should be repaired as early as possible, before the pulmonary hypertension becomes persistent.
3. Careful postoperative management is required to control the pulmonary blood flow, especially with a concomitant SP shunt.
4. Preoperative AVVR should be definitively repaired to avoid residual postoperative AVVR.

This study has some limitations. It is a retrospective review of medical records in a relatively small population. A prospective randomized trial is required to further evaluate the surgical risk factors in detail.

In conclusion, we identified TAPVC III, IV, and pulmonary atresia as risk factors for early postoperative death. Prevention of postoperative PVO is important, and intensive intervention, including perioperative management and operation, is required in this complex group of patients.

References

1. Serraf A, Bensari N, Houyel L, et al. Surgical management of congenital heart defects associated with heterotaxy syndrome. Eur J Cardiothorac Surg 2010;38:721–7.
2. Foerster SR, Gauvreau K, McElhinney DB, Geva T. Importance of totally anomalous pulmonary venous connection and postoperative pulmonary vein stenosis in outcomes of heterotaxy syndrome. Pediatr Cardiol 2008;29:536–44.
3. Stamm C, Friehs I, Duebener LF, et al. Improving results of the modified Fontan operation in patients with heterotaxy syndrome. Ann Thorac Surg 2002;74:1967–78.
4. Anagnostopoulos PV, Pearl JM, Octave C, et al. Improved current era outcomes in patients with heterotaxy syndromes. Eur J Cardiothorac Surg 2009;35:871–8.
5. Hashmi A, Abu-Sulaiman R, McCrindle BW, Smallhorn JF, Williams WG, Freedom RM. Management and outcomes of right atrial isomerism: a 26-years experience. J Am Coll Cardiol 1998;31:1120–6.
6. Hancock Friesen CL, Zurakowski D, Thiagarajan RR, et al. Total anomalous pulmonary venous connection: an analysis of current management strategies in a single institution. Ann Thorac Surg 2005;79:596–606.
7. Karamlou T, Gurofsky R, Al Sukhni E, et al. Factors associated with mortality and reoperation in 377 children with total anomalous pulmonary venous connection. Circulation 2007;115:1591–8.
8. Smallhorn JF, Burrows P, Wilson G, Coles J, Gilday DL, Freedom RM. Two-dimensional and pulsed Doppler echocardiography in the postoperative evaluation of total anom-

alous pulmonary venous connection. Circulation 1987;76: 298–305.

9. Seale AN, Uemura H, Webber SA, et al. Total anomalous pulmonary venous connection: morphology and outcome from an international population-based study. Circulation 2010;122:2718–26.

10. Jang SI, Song JY, Kim SJ, et al. The recent surgical results of total pulmonary venous return. Korean Circ J 2010;40:31–5.

11. Curzon CL, Milford-Beland S, Li JS, et al. Cardiac surgery in infants with low birth weight is associated with increased mortality: analysis of the Society of Thoracic Surgeons Congenital Heart Database. J Thorac Cardiovasc Surg 2008;135: 546–51.

12. Reddy VM, McElhinney DB, Sagrado T, Parry AJ, Teitel DF, Hanley FL. Results of 102 cases of complete repair of congenital heart defects in patients weighting 700 to 2500 grams. J Thorac Cardiovasc Surg 1999;117:324–31.

13. Caldarone CA, Najm HK, Kadletz M, et al. Surgical management of total anomalous pulmonary venous drainage: impact of coexisting cardiac anomalies. Ann Thorac Surg 1998;66:1521–6.

14. Yun TJ, Al-Radi OO, Adatia I, et al. Contemporary management of right atrial isomerism: effect of evolving therapeutic strategies. J Thorac Cardiovasc Surg 2006;131:1108–13.

15. Nakata T, Fujimoto Y, Hirose K, et al. Functional single ventricle with extracardiac total anomalous pulmonary venous connection. Eur J Cardiothoracic Surg 2009;36:49–56.

16. Yoshimura N, Oshima Y, Henaine R, Matsuhisa H. Sutureless pericardial repair of total anomalous pulmonary venous

17. Takeuchi K, Murakami A, Hirata Y, Kitahori K, Doi Y, Takamoto S. Surgical outcome of heterotaxy syndrome in a single institution. Asian Cardiovasc Thorac Ann 2006;14: 489–94.

18. Gaynor JW, Collins MH, Rychik R, Gaughan JP, Spray TL. Long-term outcome of infants with single ventricle and total anomalous pulmonary venous connection. J Thorac Cardiovasc Surg 1999;117:506–14.

19. Kim SJ, Kim WH, Lim HG, Lee CH, Lee JY. Improving results of the fontan procedure in patients with heterotaxy syndrome. Ann Thorac Surg 2006;82:1245–51.

20. Saiki H, Senzaki H. Basic concepts of circulatory physiology in congenital heart disease: a view from pressure-volume relationship. Pediatr Cardiol Cardiac Surg 2011;27:76–87.

21. Kelle AM, Backer CL, Gossett JG, Kaushal S, Mavroudis C. Total anomalous pulmonary venous connection: results of surgical repair of 100 patients at a single institution. J Thorac Cardiovasc Surg 2010;139:1387–94.

22. Ricci M, Elliott M, Cohen GA, et al. Management of pulmonary venous obstruction after correction of TAPVC: risk factors for adverse outcome. Eur J Cardiothoracic Surg 2003;24:28–36.

23. Lacour-Gayet F, Zoghbi J, Serraf AE, et al. Surgical management of progressive pulmonary venous obstruction after repair of total anomalous pulmonary venous connection. J Thorac Cardiovasc Surg 1999;117:679–87.

connection in patients with right atrial isomerism. Interact CardioVasc Thorac Surg 2010;10:675–8.

Member and Individual Subscriber Access to the Online *Annals*

The address of the electronic edition of *The Annals* is http://ats.ctsnetjournals.org. If you are an STS or STSA member or a non-member personal subscriber to the print issue of *The Annals*, you automatically have a subscription to the online *Annals*, which entitles you to access the full-text of all articles. To gain full-text access, you will need your **CTSNet user name and password**.

Society members and non-members alike who do not know their CTSNet user name and password should follow the link "Forgot your user name or password?" that appears below the boxes where you are asked to enter this information when you try to gain full-text access. Your user name and password will be e-mailed to the e-mail address you designate.

In lieu of the above procedure, if you have forgotten your CTSNet username and/or password, you can always send an email to CTSNet via the feedback button from the left navigation menu on the homepage of the online *Annals* or go directly to http://ats.ctsnetjournals.org/cgi/feedback.

We hope that you will view the online *Annals* and take advantage of the many features available to our subscribers as part of the CTSNet Journals Online. These include inter-journal linking from within the reference sections of *Annals'* articles to over 350 journals available through the HighWire Press collection (HighWire provides the platform for the delivery of the online *Annals*). There is also cross-journal advanced searching, eTOC Alerts, Subject Alerts, Cite-Track, and much more. A listing of these features can be found at http://ats.ctsnetjournals.org/help/features.dtl.

We encourage you to visit the online *Annals* at http://ats.ctsnetjournals.org and explore.

ORIGINAL ARTICLE

Heart Failure

Effect of Carvedilol on Heart Failure in Patients With a Functionally Univentricular Heart

Naoko Ishibashi, MD; In-Sam Park, MD; Tadashi Waragai, MD; Tadahiro Yoshikawa, MD;
Yasuo Murakami, MD; Katsuhiko Mori, MD; Shigekazu Mimori, MD;
Makoto Ando, MD; Yukihiro Takahashi, MD; Shouzaburo Doi, MD;
Shuuki Mizutani, MD; Toshio Nakanishi, MD

Background: The effect of carvedilol on heart failure (HF) in patients with a functionally univentricular heart (UVH) remains unclear.

Methods and Results: Carvedilol was used to treat HF in 51 patients with a UVH, classified into 3 groups: after the Fontan operation (F), after the bidirectional Glenn operation (G), and patients who had not undergone Fontan or Glenn operation (NF). Carvedilol therapy was started at a mean age of 10 ± 12 years (range: 1 month to 34 years). The initial and maximum doses of carvedilol were 0.04 ± 0.03 and $0.42\pm0.29\,mg\cdot kg^{-1}\cdot day^{-1}$, respectively. After a mean follow-up of 11 months, the cardiothoracic ratio improved from 60 ± 8 to $58\pm8\%$ (P<0.01), and the dosage of furosemide was reduced from 1.4 ± 0.9 to $0.7\pm0.7\,mg\cdot kg^{-1}\cdot day^{-1}$ (P<0.01). The ejection fraction also improved from 35 ± 12 to $40\pm11\%$ (P<0.05), and this improvement was prominent in the F group (from 35 ± 15 to $45\pm9\%$; P<0.05). Clinical signs, symptoms, and New York Heart Association functional class also improved.

Conclusions: Carvedilol may play an important role in treating HF associated with a UVH. (*Circ J* 2011; **75:** 1394–1399)

Key Words: Carvedilol; Heart failure; Univentricular heart

Since Waagstein et al first reported the use of β-blockers for the treatment of heart failure (HF) in 1975,[1] there has been increasing evidence that they improve the cardiac function and prolong survival in adult patients with HF.[2–4] Carvedilol especially, which is a nonselective β-blocker with additional vasodilatory properties, has been shown to reduce morbidity and mortality in adults with HF,[5–7] and is currently a first-line therapy for symptomatic HF in adults.[8,9]

The effectiveness of carvedilol in pediatric patients with dilated cardiomyopathy, ischemic heart disease, and congenital heart disease has been reported,[10–14] although another study failed to identify clinical effectiveness in children and adolescents with systolic HF.[15] To our knowledge, there are no reports describing the use of carvedilol for patients with a functionally univentricular heart (UVH), except for our previous case report.[16] In this study, we retrospectively evaluated the clinical effects of carvedilol for HF in patients with a UVH.

Methods

Patients

UVH in the present study included the following: single right ventricle (RV), single left ventricle (LV), tricuspid atresia, hypoplastic left heart syndrome, and complex heart diseases in which biventricular repair was not possible. Among patients admitted to hospital between 2002 and 2008, we identified 51 patients with UVH who were treated with carvedilol for HF. The anatomical diagnoses of these patients are shown in Table 1.

The definition of HF was the presence of cardiac symptoms and moderately or severely reduced ventricular systolic function. Easy fatigability, dyspnea, and/or edema were the main cardiac symptoms. Systolic ventricular dysfunction was defined as an ejection fraction (EF) $\le 50\%$, which was evaluated using 2-dimensional (D) echocardiography, in subjects in whom the anatomical LV was the main systemic chamber. In subjects in whom the RV was the main systemic chamber, systolic ventricular dysfunction was defined as the presence

Table 1. Baseline Characteristics of the UVH Patients (n=51)

	Overall	F group	G group	NF group
n	51	18	14	19
M/F	32/19	10/8	10/4	12/7
Median age	10.1 y (1 m–34.8 y)	9.5 y (1.5–30.7 y)	10.6 y (5 m–34.8 y)	10.0 y (1 m–30.1 y)
Diagnosis				
SRV	21	8	3	10
SLV	4	2	1	1
DORV	9	3	4	2
HLHS	6	2	2	2
TA	4	2		2
Other	7	1	4	2
Heterotaxia	13	5	1	7

Other includes complete atrioventricular septal defect (n=3), pulmonary atresia with intact ventricular septum (n=2), transposition of the great arteries (n=1), corrected transposition of the great arteries (n=1).
UVH, functionally univentricular heart; F group, after Fontan operation; G group, after bidirectional Glenn but before Fontan; NF group, after shunt operation or no operation; y, years; m, months; SRV, single right ventricle; SLV, single left ventricle; DORV, double-outlet right ventricle; HLHS, hypoplastic left heart syndrome; TA, tricuspid atresia.

Table 2. Dose of Carvedilol and Follow-up Duration After Reaching Maintenance Dose

	Overall cohort	F group	G group	NF group
Dose (mg·kg⁻¹·day⁻¹)				
Initial	0.04±0.03 (0.01–0.18)	0.03±0.02 (0.01–0.06)	0.04±0.02 (0.02–0.09)	0.06±0.05 (0.01–0.18)
Maximum	0.42±0.29 (0.01–0.92)	0.39±0.30 (0.06–0.82)	0.50±0.31 (0.02–0.92)	0.34±0.28 (0.01–0.78)
Follow-up (months)	11±5 (1–48)	11±3 (2–18)	12±11 (1–48)	9±5 (1–18)

Dose (mg·kg^{-1}·day^{-1}), Follow-up (months) rows as above.

Abbreviations see in Table 1.

Table 3. Clinical Parameters Before and After Administration of Carvedilol

Parameter	n	Baseline	Post-treatment	P value
CTR (%)	48	60±8	58±8	<0.01
EDP (mmHg)	15	12±5	12±4	NS
CVP (mmHg)	17	16±6	14±3	NS
EF (%)	20	35±12	40±11	<0.05
Qs (L·min⁻¹·m⁻²)	11	6±3	6±3	NS
BNP (pg/ml)	14	352±466	329±542	NS
Furosemide (mg·kg⁻¹·day⁻¹)	49	1.4±0.9	0.7±0.7	<0.01

CTR, cardiothoracic ratio; EDP, end-diastolic pressure; CVP, central venous pressure; EF, ejection fraction; Qs, systemic blood flow; BNP, serum brain natriuretic peptide.

of qualitative evidence of a dilated ventricle with moderate to severe systemic ventricular systolic dysfunction, which was evaluated using 2-D echocardiography.

The indication of carvedilol was the presence of HF, defined as above, despite the use of diuretics, digoxin, and/or angiotensin-converting enzyme (ACE) inhibitors. Firstly, we analyzed the clinical data of all the patients before and after carvedilol administration. Secondly, we analyzed the clinical data for 3 groups (ie, after Fontan operation (group F, n=18), after bidirectional Glenn but before Fontan operation (group G, n=14), and after shunt or no operation (group NF, n=19)) because the hemodynamics before the Fontan operation and after the Glenn or Fontan operation are very different.
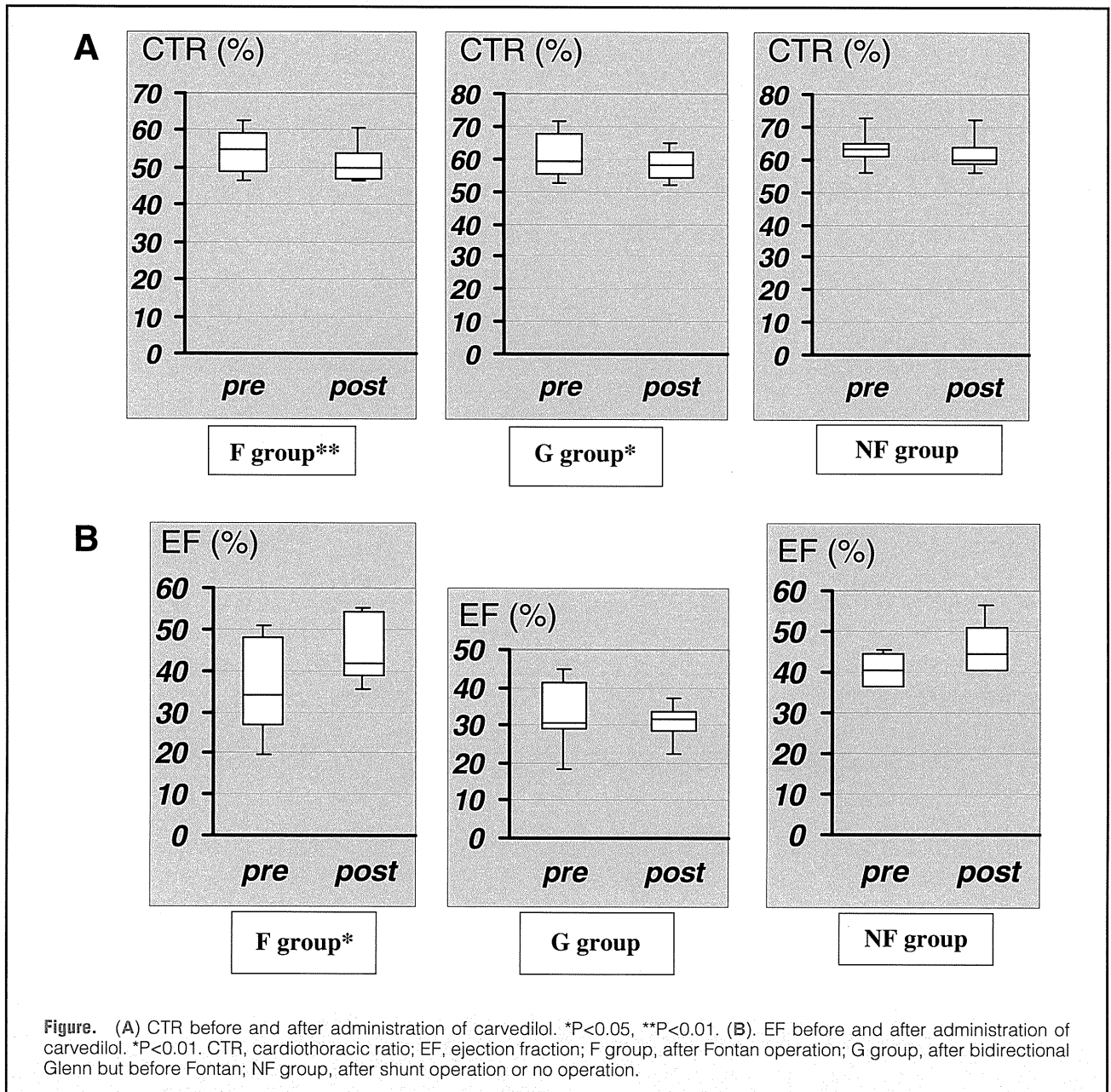
The dose of carvedilol varied according to each patient's condition, but it was basically increased to the maintenance dose within 3 months as follows: 0.05, 0.1, 0.2, 0.4, 0.6, and 0.8 mg·kg⁻¹·day⁻¹, with an increase every 2 weeks, unless HF deteriorated. The mean initial and maximum doses of carvedilol were 0.04±0.03 (0.01–0.18) and 0.42±0.29 (0.01–0.92)

mg·kg⁻¹·day⁻¹, respectively. Follow-up reaching the maintenance dose is shown in Table 2.

We compared baseline and post-treatment parameters to assess the effectiveness of carvedilol. The post-treatment parameters were obtained after reaching the maintenance dose and included the cardiothoracic ratio (CTR), ventricular end-diastolic pressure (EDP), central venous pressure (CVP), ventricular EF, systemic blood flow (Qs), ratio of pulmonary blood flow/systemic blood flow (Qp/Qs), serum brain natriuretic peptide level (BNP), and total dose of diuretic or furosemide. The EDP, CVP, EF, Qs, and Qp/Qs were measured at the time of cardiac catheterization. In patients who underwent cardiac catheterizations, the EF of the main ventricle was measured from cineangiograms using Simpson's rule.[3] We also evaluated the New York Heart Association (NYHA) functional class.

Statistical Analysis

Analysis was performed using statistical software (Excel

Figure. (A) CTR before and after administration of carvedilol. *P<0.05, **P<0.01. (B). EF before and after administration of carvedilol. *P<0.01. CTR, cardiothoracic ratio; EF, ejection fraction; F group, after Fontan operation; G group, after bidirectional Glenn but before Fontan; NF group, after shunt operation or no operation.

Statistical Program File ystat 2008.xls) for Windows, and the values are presented as the mean±standard deviation. The significance of changes in parameters was analyzed using the Wilcoxon rank sum test. P<0.05 was considered significant.

Results

Carvedilol administration was discontinued in one patient at a dose of $0.064\,mg \cdot kg^{-1} \cdot day^{-1}$ due to worsening HF, but the clinical parameters before stopping carvedilol were included in the analysis. None of the remaining patients experienced adverse effects requiring reduction in the carvedilol dose.

The numbers of patients in whom we could obtain clinical parameters are shown in Table 3. The CTR, EF, and dose of furosemide changed significantly (P<0.05) (Table 3, Figure). The EDP, Qs, and CVP did not show significant changes. With in-group analysis, the EF improved in the F group

from 35±15% (15–50%) to 45±10% (33–56%) (P<0.05), but remained unchanged in the G and NF groups. In the NF and G group (n=5), Qp/Qs before carvedilol (0.8±0.5) did not change significantly after carvedilol (1.1±0.5). The BNP improved only in the NF group from 697±639 to 373±514 pg/ml (P<0.05). The NYHA functional class, evaluated in 15 patients over 15 years of age, improved significantly (Table 4).

The main ventricular chamber was the RV in 39 patients and the LV in 12 patients. The effect of ventricular morphology on the effectiveness of carvedilol was evaluated (Table 5). Although CTR and EF improved only in patients with RV morphology, BNP improved only in patients with LV morphology.

The patients were receiving various combinations of medication (Table 6). Before starting carvedilol, 41 patients received furosemide and 13 received hydrochlorothiazide.

Table 4. NYHA Functional Class (Patients ≥15 Years)

NYHA	Baseline	Post-treatment
All patients		
II	1	11**
III	13	4
IV	1	0
F group		
II	1	5*
III	4	0
IV	0	0
G group		
II	0	2
III	2	1
IV	1	0
NF group		
II	0	4
III	7	3
IV	0	0

**P<0.01, *P<0.05.
NYHA, New York Heart Association. Other abbreviations see in Table 1.

Table 6. Medications Other Than Carvedilol

	Baseline	Post-treatment
Furosemide	41	35
Hydrochlorothiazide	13	3
Spironolactone	39	20
Enalapril	34	24
Pimobendan	9	9
Digoxin	19	8
Losartan potassium	1	2
Anti-arrhythmic agents		
Procainamide hydrochloride	1	2
Disopyramide		2
Amiodarone hydrochloride		2
Cibenzoline succinate		1

Table 5. Morphology of the Main Ventricular Chamber and Clinical Parameters Before and After Administration of Carvedilol

Parameter	Main ventricular chamber	n	Baseline	Post-treatment	P value
CTR (%)	RV	38	60±9	58±9	<0.01
	LV	10	61±7	59±4	NS
EDP (mmHg)	RV	12	11±6	12±4	NS
	LV	3	14±3	11±5	NS
CVP (mmHg)	RV	12	16±6	15±4	NS
	LV	5	17±9	13±2	NS
EF (%)	RV	12	34±13	40±12	<0.01
	LV	8	40±14	42±13	NS
BNP (pg/ml)	RV	9	450±565	490±638	NS
	LV	5	181±166	45±38	<0.05
Furosemide (mg·kg⁻¹·day⁻¹)	RV	39	1.5±1	0.8±0.9	<0.01
	LV	10	1.2±1	0.3±0.5	<0.05

RV, right ventricle; LV, left ventricle. Other abbreviations see in Table 3.

After treatment, furosemide and hydrochlorothiazide were completely discontinued in 6 and 10 patients, respectively.

Five patients died during follow-up (2 patients in the G group and 3 in the NF group). In the first patient, we had started carvedilol after the Glenn procedure, but the patient died following total cavopulmonary connection (TCPC) completion due to postoperative infection. The second patient died after the Glenn procedure due to postoperative infection. In the third patient, carvedilol had to be discontinued due to renal failure caused by cyanotic nephropathy. In the fourth patient, we had started carvedilol following the initial Norwood operation, but the patient died of aggravating subsemilunar valve stenosis. The fifth patient died of bacterial endocarditis. None of these deaths was attributable to the side-effects of carvedilol.

Discussion

We have reported a previous case in which carvedilol was effective for HF that developed after the Fontan operation.[16] That patient had severe cardiac failure (NYHA class III), but underwent a successful TCPC conversion operation after improvement in cardiac function following carvedilol therapy. This experience prompted us to use carvedilol in a series of patients with UVH suffering from HF.

Beta-blockers have been shown to decrease mortality and morbidity in adult clinical trials, promising to markedly advance the treatment of HF.[17] They enhance ventricular remodeling,[18–20] decrease the levels of free radicals[21–23] and adverse neurohumoral factors,[24–27] decrease arrhythmia, and thus reduce HF symptoms.[9,28–30]

In this study, the CTR and EF were improved and the total dose of diuretics was decreased by carvedilol therapy. The EF particularly improved in the F group. When we focused on the group of patients ≥15 years, improvement in NYHA class was observed, although the mechanisms of this improvement remains unclear. In particular, the effect of carvedilol on diastolic ventricular function remains to be clarified.

In the study by Shaddy et al[15] of pediatric patients in whom the main chamber was the LV, the LV shortening fraction increased in the placebo group, low-dose (0.2mg/kg) carvedilol group, and high-dose (0.4mg/kg) carvedilol group, but the increase was the greatest in the high-dose carvedilol group. Their study results suggested a beneficial trend in high-dose carvedilol therapy in patients in whom the main chamber was the LV. In the present study, such dose dependency could not be analyzed because of the small number of patients. Patients in the other study consisted mainly of those with dilated cardiomyopathy, whereas we did not include such patients in the present study and the majority of patients had the RV as the main chamber. In the present study, the chamber-specific tendency was heterogeneous (Table 5). Although CTR and EF improved only in patients with RV morphology, BNP improved only in patients with LV morphology. The reasons why the changes in parameters were not consistent in the present study remain unclear, but the different response to carvedilol by the 2 ventricles may be 1of the reasons. The present study, however, did show that carvedilol is effective in patients with the RV as the main chamber.

Serum BNP levels have shown by some to be useful for evaluating cardiac function in the UVH in some reports,[31-35] but not by others.[36] In the present study, the BNP level did not show a significant change in Fontan patients despite improvements in some of the clinical parameters. The reason for this remains unclear, and so future follow-up is necessary.

Study Limitations

Firstly, this study is a retrospective analysis of the effects of carvedilol for HF in patients with a UVH and therefore the degree of ventricular dysfunction was not identical among subjects. Secondly, systolic ventricular dysfunction was determined using echocardiography. Calculation of the EF of the RV from echocardiography in the UVH is difficult and therefore RV function was evaluated qualitatively. In previous studies investigating the effect of carvedilol in patients with cardiomyopathy and congenital heart diseases, including UVH, RV function was also evaluated in a similar fashion.[15,37] Thirdly, the subjects had heterogeneous diagnoses. Multiple operations were carried out over the course of carvedilol treatment, as is often required in patients with a UVH. These factors may have influenced cardiac function, aside from the pharmacological effects of carvedilol. In the present study, however, the effect of carvedilol was evaluated within the group before and after operations. Fourthly, the relationship between the dose of carvedilol and its effectiveness remains unclear. In the present study, post-treatment clinical parameters were obtained after reaching the maintenance dose because clinical evaluation during dose adjustment was difficult.

Conclusions

This study demonstrated that the addition of carvedilol to standard medical treatments such as diuretics, digoxin, and ACE inhibitor could reduce the symptoms of HF and improve clinical parameters in patients with a UVH. Multicenter, randomized, controlled, prospective trials are mandatory to further elucidate the effect of carvedilol in the treatment of HF in patients with a UVH.

References

1. Waagstein F, Hjalmarson A, Varnauskas E, Wallentin I. Effect of chronic beta-adrenergic receptor blockade in congestive cardiomy-
opathy. Br Heart J 1975; 37: 1022–1036.
2. Swedberg K, Hjalmarson A, Waagstein F, Wallentin I. Prolongation of survival in congestive cardiomyopathy by beta-receptor blockade. Lancet 1979; 1: 1374–1376.
3. Mortara A, Rovere M, Pinna G, Maestri R, Capomolla S, Cobelli F. Nonselective beta-adrenergic blocking agent, carvedilol, improves arterial baroflex gain and heart rate variability in patients with stable chronic heart failure. J Am Coll Cardiol 2000; 36: 1612–1618.
4. Beta-Blocker Evaluation of Survival Trial Investigators. A trial of the beta-blocker bucindolol in patients with advanced chronic heart failure. N Engl J Med 2001; 344: 1659–1667.
5. Packer M, Bristow M, Cohn J, Colucci WS, Fowler MB, Gilbert EM, et al. The effect of carvedilol on morbidity and mortality in patients with chronic heart failure. N Engl J Med 1996; 334: 1349–1355.
6. Whorlow S, Krum H. Meta-Analysis of effect of beta-blocker therapy on mortality in patients with New York heart association class IV chronic congestive heart failure. Am J Cardiol 2000; 86: 886–889.
7. Packer M, Coats A, Fowler M, Katus HA, Krum H, Mohacsi P, et al; Carvedilol Prospective Randomized Cumulative Survival Study Group. Effect of carvedilol on survival in severe chronic heart failure. N Engl J Med 2001; 344: 1651–1658.
8. Packer M, Colucci W, Sackner-Bernstein J, Liang CS, Goldscher DA, Freeman I, et al. Double-blind, placebo-controlled study of the effects of carvedilol in patients with moderate to severe heart failure: The PRECISE trial [Prospective Randomized Evaluation of Carvedilol on Symptoms and Exercise]. Circulation 1996; 94: 2793–2799.
9. Colucci W, Packer M, Bristow M, Gilbert EM, Cohn JN, Fowler MB, et al. Carvedilol inhibits clinical progression in patients with mild symptoms of heart failure: US Carvedilol Heart Failure Study Group. Circulation 1996; 94: 2800–2806.
10. Buchhorn R, Bartmus D, Siekmeyer W, Hulpe-Wette M, Schulz R, Bursch J. Beta-blocker therapy of severe congestive heart failure in infants with left to right shunts. Am J Cardiol 1998; 81: 1366–1368.
11. Bruns L, Chrisant M, Lamour J, Shaddy RE, Pahl E, Blume ED, et al. Carvedilol as therapy in pediatric heart failure: An initial multicenter experience. J Pediatr 2001; 138: 505–511.
12. Laer S, Mir T, Behn F, Eiselt H, Venzke A, Meibohm B, et al. Carvedilol therapy in pediatric patients with congestive heart failure: A study investigating clinical and pharmacokinetic parameters. Am Heart J 2002; 143: 916–922.
13. Giardini A, Formigari R, Bronzetti G, Prandstraller D, Donti A, Bonvicini M, et al. Modulation of neurohormonal activity after treatment of children in heart failure with carvedilol. Cardiol Young 2003; 13: 333–336.
14. Blume E, Canter C, Spicer R, Gauvreau K, Colan S, Jenkins KJ. Prospective single-arm protocol of carvedilol in children with ventricular dysfunction. Pediatr Cardiol 2006; 27: 336–342.
15. Shaddy R, Boucek M, Hsu D, Boucek RJ, Canter CE, Mahony L, et al. Carvedilol for children and adolescents with heart failure: A randomized controlled trial. JAMA 2007; 298: 1171–1179.
16. Ishibashi N, Park I, Takahashi Y, Nishiyama M, Murakami Y, Mori K, et al. Effectiveness of carvedilol for congestive heart failure that developed long after modified Fontan operation. Pediatr Cardiol 2006; 27: 473–475.
17. Olsen S, Gilbert E, Renlund DG, Taylor DO, Yanowitz FD, Bristow MR. Carvedilol improves left ventricular function and symptoms in chronic heart failure: A double-blind randomized study. J Am Coll Cardiol 1995 25: 1225–1231.
18. Groenning B, Nilsson J, Sondergaard L, Fritz-Hansen T, Larsson HB, Hildebrandt PR. Antiremodeling effects on the left ventricle during beta-blockade with metoprolol in the treatment of chronic heart failure. J Am Coll Cardiol 2000; 36: 2072–2080.
19. Kubo H, Margulies K, Piacentino V 3rd, Gaughan JP, Houser SR. Patients with end-stage congestive heart failure treated with β-adrenergic receptor antagonists have improved ventricular myocyte calcium regulatory protein abundance. Circulation 2001; 104: 1012–1018.
20. Reiken S, Wehrens X, Vest J, Barbone A, Klotz S, Mancini D, et al. Beta-blockers restore calcium release channel function and improve cardiac muscle performance in human heart failure. Circulation 2003; 107: 2459–2466.
21. Keith M, Geranmayegan A, Sole M, Kurian R, Robinson A, Omran AS, et al. Increased oxidative stress in patients with congestive heart failure. J Am Coll Cardiol 1998; 31: 1352–1356.
22. Flesch M, Maack C, Cremers B, Bäumer AT, Südkamp M, Böhm M. Effect of beta-blockers on free radical-induced cardiac contractile dysfunction. Circulation 1999; 100: 346–353.

23. Arumanayagam M, Chan S, Tong S, Sanderson JE. Antioxidant properties of carvedilol and metoprolol in heart failure: A double-blind randomized controlled trial. *J Cardiovasc Pharmacol* 2001; **37:** 48–54.

24. Gilbert E, Abraham W, Olsen S, Hattler M, White M, Mealy P, et al. Comparative hemodynamic, left ventricular functional, and anti-adrenergic effects of chronic treatment with metoprolol versus carvedilol in the failing heart. *Circulation* 1996; **94:** 2817–2825.

25. Prabhu S, Chandrasekar B, Murray D, Freeman GL. Beta-adrenergic blockade in developing heart failure: Effects on myocardial inflammatory cytokines, nitric oxide and remodeling. *Circulation* 2000; **101:** 2103–2109.

26. Dandona P, Karne R, Ghanim H, Hamouda W, Aljada A, Magsino CH Jr. Carvedilol inhibits reactive oxygen species generation by leukocytes and oxidative damage to amino acids. *Circulation* 2000; **101:** 122–124.

27. Nishiyama K, Tsutamoto T, Yamaji M, Kawahara C, Yamamoto T, Fujii M, et al. Dose-dependent prognostic effect of carvedilol in patients with chronic heart failure: Special reference to ranscardiac gradient of norepinephrine. *Circ J* 2009; **73:** 2270–2275.

28. Lowes B, Gill E, Abraham W, Larrain JR, Robertson AD, Bristow MR, et al. Effects of carvedilol on left ventricular mass, chamber geometry, and mitral regurgitation in chronic heart failure. *Am J Cardiol* 1999; **83:** 1201–1205.

29. Capomolla S, Febo O, Gnemmi M, Riccardi G, Opasich C, Caporotondi A, et al. Beta-blockade therapy in chronic heart failure: Diastolic function and mitral regurgitation improvement by carvedilol. *Am Heart J* 2000; **139:** 596–608.

30. Yamaji M, Tsutamoto T, Tanaka T, Kawahara C, Nishiyama K, Yamamoto T, et al. Effect of carvedilol on plasma adiponectin concentration in patients with chronic heart failure. *Circ J* 2009; **73:** 1067–1073.

31. Law Y, Ettedgui J, Beerman L, Maisel A, Tofovic S. Comparison of plasma B-type natriuretic peptide levels in single ventricle patients with systemic ventricular heart failure versus isolated cavopulmonary failure. *Am J Cardiol* 2006; **98:** 520–524.

32. Anderson P, Sleeper L, Mahony L, Colan SD, Atz AM, Breitbart RE, et al; Pediatric Heart Network Investigators. Contemporary outcomes after the Fontan procedure; A Pediatric Heart Network multicenter study. *J Am Coll Cardiol* 2008; **52:** 85–98.

33. Berry J, Askovich B, Shaddy R, Hawkins JA, Cowley CG. Prognostic value of B-type natriuretic peptide in surgical palliation of children with single-ventricle congenital heart disease. *Pediatr Cardiol* 2008; **29:** 70–75.

34. Koch A, Zink S, Singer H, Dittrich S. B-type natriuretic peptide levels in patients with functionally univentricular hearts after total cavopulmonary connection. *Eur J Heart Failure* 2008; **10:** 60–62.

35. Hsu J, Oishi P, Keller R, Chikovani O, Karl TR, Azakie A, et al. Perioperative B-type natriuretic peptide levels predict outcome after bidirectional cavopulmonary anastomosis and total cavopulmonary connection. *J Thorac Cardiovasc Surg* 2008; **135:** 746–753.

36. Larsson D, Meurling C, Holmqvist F, Waktare JE, Thilen UJ. The diagnostic and prognostic value of brain natriuretic peptide in adults with a systemic morphologically right ventricle or Fontan-type circulation. *Int J Cardiol* 2007; **114:** 345–351.

37. Auerbach SR, Richmond ME, Lamour JM, Blume ED, Addonizio LJ, Shaddy RE, et al. BNP levels predict outcome in pediatric heart failure patients. *Circ Heart Fail* 2010; **3:** 606–611.

CASE REPORT

Cardiac tamponade due to perforation by an Amplatzer atrial septal occluder in a patient with Marfan syndrome

Minori Tateishi · Takeshi Hiramatsu · Yasuko Tomizawa ·
Goki Matsumura · Takeshi Konuma · Kenji Yamazaki ·
Hideshi Yamamura · Toshio Nakanishi

Abstract Device closure of atrial septum defect was performed using an Amplatzer septal occluder in a 48-year-old patient with Marfan syndrome. Acute tamponade due to perforation was observed 2 months after catheter intervention. Careful consideration of the indication for device closure for atrium septal defect is necessary in patients with Marfan syndrome.

Keywords Atrial closing device · Catheter intervention · Marfan syndrome · Complication · Perforation

Introduction

Biocompatibility is an essential requirement for implantable artificial organs and biomaterials [1]. When used in the heart, the physical property of an implanted device and the relationship between surrounding native tissue and the implanted device are especially important [2] because the implanted device is usually solid and rigid, whereas the heart is tender and beating. Recently, transcatheter closure of atrium septal defect (ASD) using the Amplatzer septal occluder has become a therapeutic option for ASD [3, 4]. Since the first report of a Japanese clinical trial of device closure for ASD in 2002 [5], the total number of such

procedures has reached almost 2,000. However, reports of complications after device closure are limited, and comparative study of surgical and device closure of ASD is rare in Japan. We report a patient with Marfan syndrome who underwent device closure of ASD in September 2010 and experienced acute tamponade due to perforation.

Case report

A 48-year-old woman with an ASD and Marfan syndrome presented at our hospital with Qp/Qs = 3.1 and was indicated for ASD closure. Aortic valve regurgitation was mild, and she was not indicated for aortic surgery. The long and short diameters were: aortic valve 25.6 and 24.3 mm; sinus of Valsalva 40.1 and 36.0 mm; ST junction 28.1 and 26.9 mm; ascending aorta 30.6 and 30.6 mm. The patient preferred to undergo device closure and was treated successfully by placing a 30-mm Amplatzer septal occluder (AGA Medical Corporation, Golden Valley, MN, USA) under general anesthesia using transesophageal echocardiography in the catheterization laboratory. Echocardiography conducted 1 day after the procedure showed no change in device position, but pericardial effusion of 6 mm was noticed at diastole, which did not exist before the procedure. At day 6, the patient was discharged after examination revealed no further abnormalities. At the outpatient follow-up 1 month after the procedure, the patient was well, and echocardiography showed pericardial effusion of 1.3 mm at diastolic and 6 mm at systole. Two months after the procedure, she visited our hospital to collect documents in the morning and noticed increasing dyspnea during the train ride on her way home. At 1330 hours on the same day, she presented at her family doctor with orthopnea. Shock due to cardiac tamponade was diagnosed from

M. Tateishi · T. Hiramatsu · Y. Tomizawa (✉) ·
G. Matsumura · T. Konuma · K. Yamazaki
Department of Cardiovascular Surgery,
Tokyo Women's Medical University, 8-1 Kawada,
Shinjuku, Tokyo 162-8666, Japan
e-mail: 4CRNRY@hij.twmu.ac.jp

H. Yamamura · T. Nakanishi
Department of Pediatric Cardiology,
Tokyo Women's Medical University, Tokyo, Japan
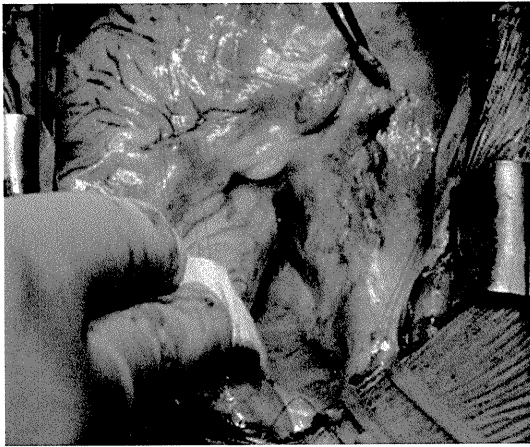
🙂 Springer

Fig. 1 View at surgery. After opening the pericardium and removing the dark red clot, no active bleeding was observed. A hematoma was found at the aortic root facing the right atrium. *Bottom* caudal side

echocardiographic findings. She was administered an inotropic agent and transported to our hospital by helicopter. She arrived at 1645 hours with hypotension and impaired consciousness. Emergency surgery was performed.

Under a midsternotomy, the pericardium was found to be filled with 500 ml of dark red clot. There was no active bleeding (Fig. 1). A hematoma was observed at the aortic wall facing the right atrium. Under extracorporeal circulation with cardiac arrest, the right atrium was opened and the device was found to be adhered to the ceiling of the right and left atria. Erosion was found at the right and left atrial roof. After the device was removed, a tear measuring 1 cm in length was found at the ceiling of both right and left atria. The color of the explanted device was whitish with red spots (Fig. 2). The tear was closed with a 4–0 Prolene suture. The arterial wall with hematoma at the aortic root was reinforced with a felt pledget. The ASD was positioned centrally with an intact superior rim 15 mm × 30 mm. An expanded polytetrafluoroethylene (ePTFE) patch 0.4-mm thick was used for closure.

The patient was discharged uneventfully on the 16th postoperative day.

Discussion

Configuration, size, shape, and stiffness of an intracardiac device have great impact on the heart after implantation. After the ASD is closed by a device, the shape and the volume of the ventricle and atrium change [6] and become smaller. Additionally, when the patient grows, residual shunt may occur due to an increase in size of the ASD [7]. Moreover, configuration of the device may be changed when the aortic root is enlarged, as in the case of Marfan syndrome. Various complications after device closure have
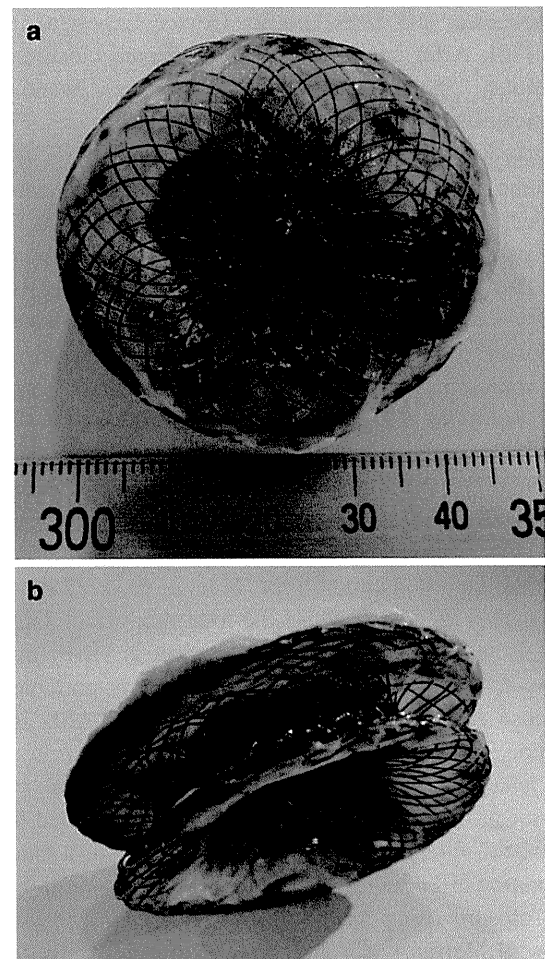

Fig. 2 Removed device: The disc positioned in the left atrium (**a**) and oblique view showing the disc (*lower*) positioned in the right atrium (**b**). The device was whitish with red spots after 2 months of implantation

been reported, such as thromboembolism, device embolization, arrhythmia, erosion, perforation, acute tamponade, and serious great-vessel injury [5, 8]. Amin et al. [8] analyzed 28 cases of hemodynamic compromise after device closure and reported that all erosions occurred at the roof of the atria, near the aortic root. In their report, 21 of 28 patients had surgery, and 16 of those 21 patients had the device removed in addition to perforation or fistula repair. Although the authors emphasized that early detection and prompt treatment are mandatory, the follow-up data of seven nonsurgical and five surgical cases without device removal were missing. Another report in 2005 pointed out that cardiac perforation occurred predominantly in the anterosuperior atrial walls and/or adjacent aorta [9].

Complications are more serious with device closure than with surgical closure. From 2002 to 2009, 223 adverse events, including 152 surgical rescue operations and 17 deaths, in patients undergoing Amplatzer ASD closure were submitted to the US Food and Drug Administration

Manufacturer and User Facility Device Experience database [10]. After surgical rescue for device closure complications, mortality rate per adverse event was significantly higher in the device closure cases (7.6%) compared with surgical closure cases (1.2%) [10]. During the same period, the Society of Thoracic Surgery database registered two deaths and six reoperations among 1,537 ASD primary operation cases [10]. Device closure cannot be called noninvasive therapy, because emergency rescue surgery may be required during or after the procedure.

Closure-device-related complications that require surgical rescue may occur even in the long term. A European study involving 19 participating institutions reviewed 56 cases of complications following device closure of ASD (1997–2007) and reported late dislodgement occurring 8 years after initial hospital discharge [11]. In Japan, no death has been reported after device closure until now (personal communication, Prof. Shun-ei Kyo, 23 February 2011). This may be because the total number of Japanese cases is still small, follow-up duration is short, and no follow-up survey has been conducted. It is possible that Japanese experience with device closure of ASD is still limited.

In Marfan syndrome, the distance from the aortic root to the roof of the right and left atria may be shortened due to aortic-root enlargement, which may constitute a cause of perforation after device closure. A case of penetration after ASD closure using an Amplatzer device in a 9-year-old boy with Marfan syndrome was reported [12]. The aortic root was 24 mm at the time of device closure but grew to 30 mm 2 years later. In this case, the device was removed surgically, the ASD closed, and the aortic sinus reconstructed [12]. It is important to predict the possible clinical course after device closure.

Adverse events after device closure occur suddenly, without any warning sign after hospital discharge, and over the long term. Hence, device closure of ASD is not a low-risk procedure because follow-up for as long as 10–15 years is required. At this point, a survey of implanted closing devices in patients in Japan is warranted.

Conclusion

Careful consideration of the indication of device closure for ASD is necessary in patients with Marfan syndrome.

References

1. Tateishi M, Tomizawa Y. Intravascular foreign bodies: danger of unretrieved fragmented medical devices. J Artif Organs. 2009;12:80–9.
2. Sawa Y, Tatsumi E, Funakubo A, Horiuchi T, Iwasaki K, Kishida A, Masuzawa T, Matsuda K, Myoui A, Nishimura M, Nishimura T, Tomizawa Y, Tomo T, Yamaoka T, Watanabe H. Journal of artificial organs 2009: the year in review. J Artif Organs. 2010;13:1–9.
3. Masura J, Gavora P, Formanek A, Hijazi ZM. Transcatheter closure of secundum atrial septal defects using the new self-centering amplatzer septal occluder: initial human experience. Cathet Cardiovasc Diagn. 1997;42:388–94.
4. Yasukochi S. Current status of transcatheter closure of atrial septal defect. Respir Circ. 2009;57:1305–10 (in Japanese).
5. Oho S, Ishizawa A, Akagi T, Dodo H, Kato H. Transcatheter closure of atrial septal defects with the Amplatzer septal occluder: a Japanese clinical trial. Circ J. 2002;66:791–4.
6. Dhillon R, Josen M, Henein M, Redington A. Transcatheter closure of atrial septal defect preserves right ventricular function. Heart. 2002;87:461–5.
7. Zhu W, Neubauer H. Secondary residual shunt after atrial septal defect closure with an amplatzer occluder: surgical removal and evaluation of device biocompatibility after 7 years. Pediatr Cardiol. 2010;31:1107–10.
8. Amin Z, Hijazi ZM, Bass JL, Cheatham JP, Hellenbrand WE, Kleinman CS. Erosion of Amplatzer septal occluder device after closure of secundum atrial septal defects: review of registry of complications and recommendations to minimize future risk. Cathet Cardiovasc Interv. 2004;63:496–502.
9. Divekar A, Gaamangwe T, Shaikh N, Raabe M, Ducas J. Cardiac perforation after device closure of atrial septal defects with the Amplatzer septal occluder. J Am Coll Cardiol. 2005;45:1213–8.
10. DiBardino DJ, McElhinney DB, Kaza AK, Mayer JE Jr. Analysis of the US Food and Drug Administration Manufacturer and User Facility Device Experience database for adverse events involving Amplatzer septal occluder devices and comparison with the Society of Thoracic Surgery congenital cardiac surgery database. J Thorac Cardiovasc Surg. 2009;137:1334–41.
11. Sarris GE, Kirvassilis G, Zavaropoulos P, Belli E, Berggren H, Carrel T, Comas JV, Corno AF, Daenen W, Di Carlo D, Ebels T, Fragata J, Hamilton L, Hraska V, Jacobs J, Lazarov S, Mavroudis C, Metras D, Rubay J, Schreiber C, Stellin G. Surgery for complications of trans-catheter closure of atrial septal defects: a multi-institutional study from the European Congenital Heart Surgeons Association. Eur J Cardiothorac Surg. 2010;37:1285–90.
12. Loeffelbein F, Schlensak C, Dittrich S. Penetration of left and right atrial wall and aortic root by an Amplatzer atrial septal occluder in a nine year old boy with Marfan syndrome: case report. J Cardiothorac Surg. 2008;3:25.
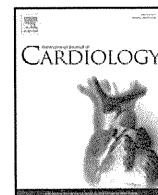
Letter to the Editor

Asynchronous contraction of the 2 ventricles caused by ventricular pacing after a Fontan-type operation in a patient with a biventricular heart

Takashi Higaki [a,c,*], Chisato Kondo [b], Hirofumi Tomimatsu [a], Eiji Yamamura [a], Eiichi Yamamoto [a,c], Kyoko Konishi [a,c], Mitsugi Nagashima [d], Toshio Nakanishi [a]

[a] Department of Pediatric Cardiology, Heart Institute of Japan, Tokyo Women's Medical University, Tokyo, Japan
[b] Department of Diagnostic Imaging and Nuclear Medicine, Tokyo Women's Medical University, Tokyo, Japan
[c] Department of Pediatric Cardiology, Stroke & Cardiovascular Center, Ehime University Hospital, Ehime, Japan
[d] Department of Cardiovascular Surgery, Stroke & Cardiovascular Center, Ehime University Hospital, Ehime, Japan

ARTICLE INFO

ABSTRACT

We treated a 6-year-old boy who had polysplenia syndrome and tetralogy of Fallot with a small right ventricle (RV), an atrial septal defect, a hemiazygos connection, and bilateral superior vena cava. Because the RV was too small for a biventricular repair to be performed, the patient underwent a total cavopulmonary shunt operation although his heart was biventricular and a pacemaker (VVI) had been implanted for management of the sick sinus syndrome complicated by polysplenia syndrome. After the operation, marked asynchronous contraction was noted between the morphological right and left ventricles and was probably responsible for the low cardiac output noted in this patient. In order to clarify the significance of the asynchronous contraction, we determined the cause of the low cardiac output by studying the time course of the volume changes in the morphological right and left ventricles during a cardiac cycle by using angiograms. In addition, we studied the interventricular flow dynamics by using pulsed-Doppler echocardiography.

After a Fontan-type operation is performed on patients with a biventricular heart, the 2 ventricles may not function in perfect coordination when they have to work as 1 unit. These patients are likely to develop cardiac dysfunction due to interventricular to-and-fro flow dynamics. Asynchronous contraction between the 2 ventricles caused by abnormal interventricular conduction impaired the cardiac performance in the present case.

© 2010 Elsevier Ireland Ltd. All rights reserved.

1. Introduction

The indications for the Fontan procedure [1,2] have been expanded beyond the original criteria [3,4] to include a wide variety of anomalies with various complications; people with biventricular hearts are also now considered as candidates for this type of operation. The 2 ventricles may not be able to work in perfect coordination when they have to function as 1 unit [5,6]. We treated a patient with a biventricular heart who had undergone a Fontan-type operation and required pacemaker implantation. After the operation, the patient developed marked asynchronous contraction between the morphological right and left ventricles

(LV), and this defect was probably responsible for the low cardiac output noted in this patient. These observations suggest that interventricular conduction abnormalities may cause asynchronous contraction. This report clarifies the significance of abnormal interventricular conduction induced by pacemaker implantation in a patient who had a biventricular heart and had undergone the Fontan-type operation; such a case has not been previously documented.

2. Case report

The patient was a 6-year-old boy diagnosed with polysplenia syndrome and tetralogy of Fallot with a small right ventricle (RV). Because of decreasing arterial oxygen saturation, the boy had undergone a Blalock–Taussig shunt operation at the age of 1 month. Because the RV was expected to increase in size over time, a pulmonary valvotomy was performed at the age of 5 years. However, 1 year later, the RV was still too small for biventricular repair; therefore, he finally underwent a total cavopulmonary shunt operation and a pacemaker (VVI) was implanted at the LV apex for management of the sick sinus syndrome complicated by polysplenia syndrome. After the operation, angiography revealed marked asynchronous contraction between the morphological RV and LV (Fig. 1A,B). Therefore,

* Corresponding author. Department of Pediatric Cardiology, Stroke & Cardiovascular Center, Ehime University Hospital, Shitsukawa, Toon, Ehime 791-0295, Japan. Tel.: +81 89 960 5320; fax: +81 89 960 5941.
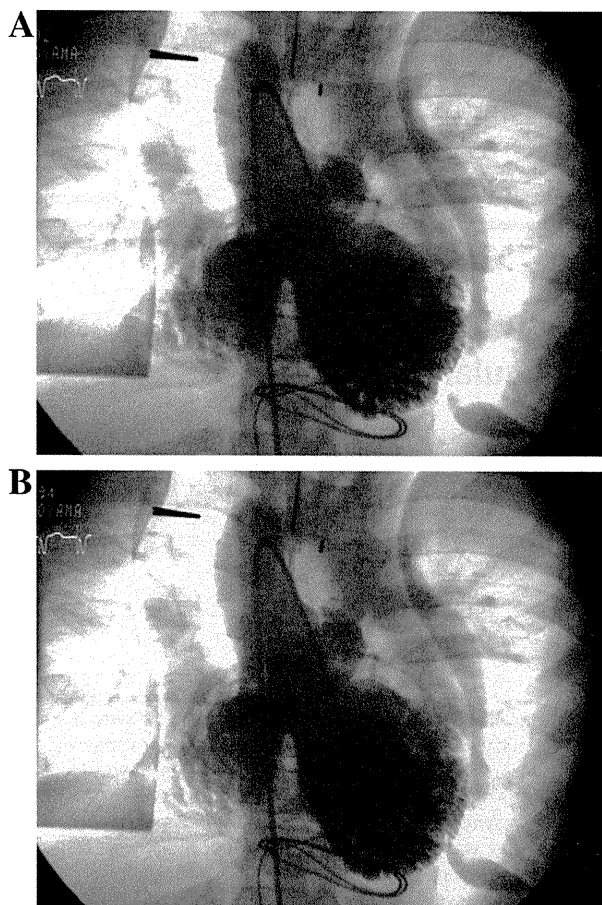E-mail address: higaki@m.ehime-u.ac.jp (T. Higaki).

Fig. 1. Angiography revealed that the cardiac cycle was asynchronous between the 2 ventricles. A, During early systole, the left ventricle (LV) is in systole while the right ventricle (RV) is still in the relaxation phase and is expanded by the output of the LV. B, This association is reversed during mid-systole: the RV begins to contract, and a fraction of the RV output flows toward the LV.

Fig. 2. The time course of volume changes in the LV and RV is shown. Notably, the 2 curves largely do not overlap. The RV is paradoxically dilated during early LV systole, and when the RV begins to contract later than the LV, the LV is paradoxically dilated during the RV contraction.

we analyzed the effect of the pacemaker on the hemodynamics and ventricular function.

2.1. Cardiac catheterization

The preoperative data revealed that the mean pulmonary artery pressure (mPAP) was 17 mm Hg; the pulmonary artery (PA) resistance, 1.8 units·m²; and the PA index, 310 mm²/m². The left ventricular end-diastolic volume (LVEDV) was 151% of the normal value, and the ejection fraction (EF) was 0.61. The right ventricular end-diastolic volume (RVEDV) was 58% of the normal value, and the EF was 0.61. After the operation, the mPAP was 13 mm Hg and the cardiac output was 2.4 l/min/m². The LVEDV was 170% of the normal value, and the EF was 0.25. The RVEDV was 78% of the normal value, and the EF was 0.52.

2.2. Electrocardiogram

An electrocardiogram (ECG) obtained after the operation, during ventricular pacing, revealed a prolonged QRS interval of 0.12 s and complete right bundle-branch block. On turning off the pacemaker, the ECG in the spontaneous cardiac rhythm showed junctional rhythm, a narrow QRS interval of 0.08 s, no bundle-branch block.

2.3. Time course of volume changes in the morphological RV and LV in a cardiac cycle

Using a biplane cine-angiogram filmed at a rate of 60 frames/s, we calculated the LV and RV volumes in each frame from one Q wave of the ECG to the next Q wave by using the area-length method and Simpson's rule, respectively. As shown in Fig. 2, the LV contracted, but paradoxically, the RV volume increased. Thereafter, the RV contracted and the LV dilated. As the RV contracted, the aortic valve opened and blood was ejected into the aorta.
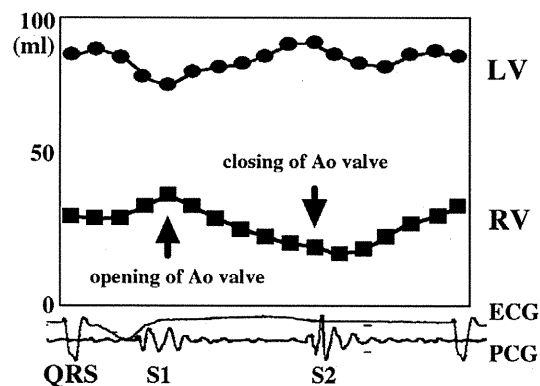
2.4. Interventricular flow dynamics as assessed using pulsed-Doppler echocardiography

The interventricular flow pattern noted during ventricular pacing showed that the LV-to-RV flow began during early LV systole after the QRS complex appeared on the ECG and persisted until around the time the first sound was recorded on the phonocardiogram, that is, the sound of the aortic valve opening. This was followed by the RV-to-LV flow, which persisted during mid-systole (Fig. 3A). When the pacemaker was turned off, the LV-to-RV flow coincided with the opening of the aortic valve and persisted throughout the systole (Fig. 3B).

3. Discussion

This study revealed that in a patient with a biventricular heart, asynchronous contraction of the 2 ventricles after the Fontan-type operation was associated with the right bundle-branch block pattern that was observed on an ECG. Asynchronous contraction resulted from pacing at the LV; that is, the LV started contracting earlier than the RV. At the time of early LV systole, the RV was still in the relaxation phase and was expanded passively owing to the LV output. The aortic valve had not yet opened by that time, and the LV output was not ejected into the aorta. Thus, the LV output was not the true cardiac output (Fig. 4A,a). When the RV started to contract later than the LV, the aortic valve opened, and the LV began to eject its output into the aorta; this was the actual cardiac output (Fig. 4A,b). However, a fraction of the RV output flowed toward the LV and affected the LV contraction (Fig. 4A,c). Thus, the interventricular bidirectional flow due to communicating ventricular septal defect led to a low total cardiac output.

In contrast, when the patient's pacemaker was turned off, the asynchronicity of the contractions disappeared. In the natural cardiac rhythm, a narrow QRS interval was associated with monophagic LV-to-RV interventricular flow (Fig. 4B).

We previously reported that asynchronous contraction of the 2 ventricles is a significant factor affecting cardiac output after the Fontan procedure in patients with a biventricular heart, especially in those with a large end-diastolic volume and low ejection fraction; however, the cause of this asynchronous contraction was not clear [6]. The results of the present study suggest that a delay in interventricular conduction causes asynchronous contraction.

A recent study described the use of cardiac resynchronization therapy (CRT) as a novel adjunctive therapy for patients with advanced heart failure [7–9]. The efficacy of CRT is based on the reduction in the conduction delay between the 2 ventricles. In the case described here, a delay in interventricular conduction was responsible for asynchronous contraction; CRT is expected to be an effective mode of therapy. However, further studies are required to assess the clinical outcome of this therapy [9].
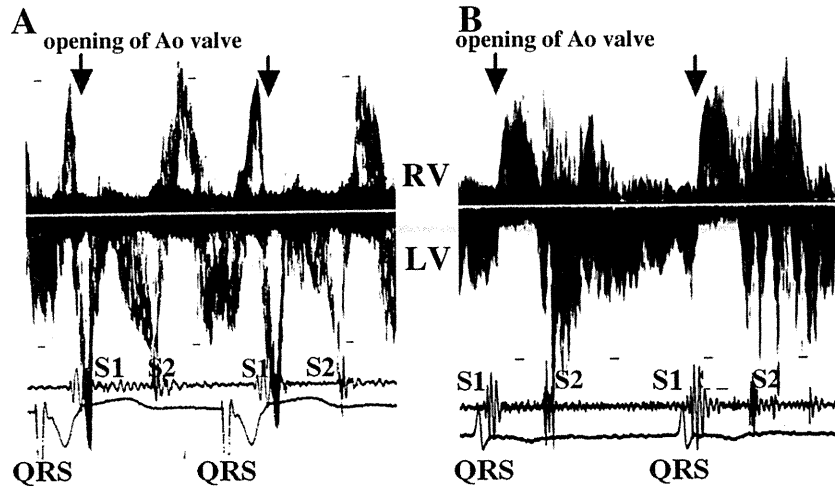
Fig. 3. The interventricular flow dynamics were studied by pulsed-Doppler echocardiography in the parasternal short-axis view with the sample volume set between the RV and LV or through the ventricular septal defect. All the recordings obtained by electrocardiography and phonocardiography were superimposed. A. Pacing at the LV: the interventricular flow pattern noted during ventricular pacing shows that the LV-to-RV flow begins during early LV systole, after the QRS complex appears on the ECG and persists until around the time the first sound is recorded on the phonocardiogram, that is, the sound of the aortic valve opening. This is followed by the RV-to-LV flow, which persists during mid-systole. B. Spontaneous cardiac rhythm: The LV-to-RV flow, coinciding with the opening of the aortic valve, persists throughout the systole. No remarkable flow occurs between the time the QRS complex appears and the time the first sound is audible.
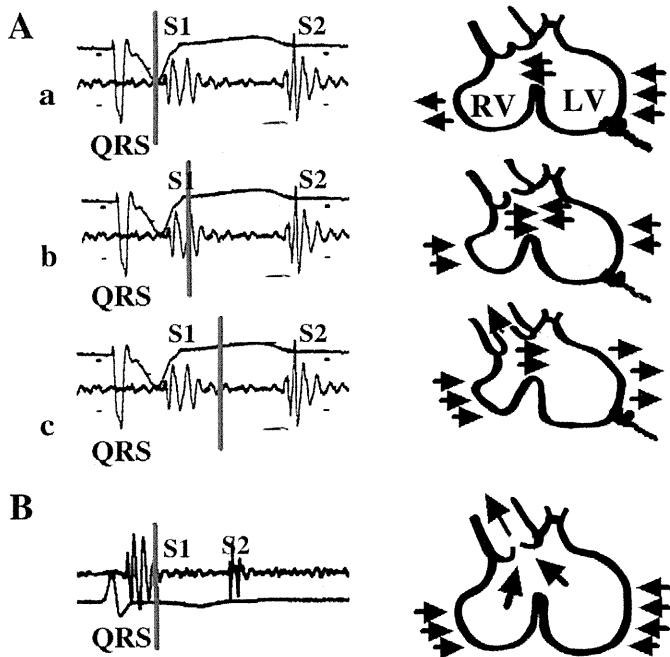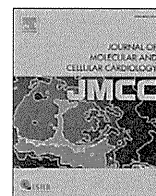

Fig. 4. Schematic illustration of the hemodynamic changes. A. Pacing at the LV apex. a. The LV begins to contract earlier than the RV. During early LV systole, the RV is still in the relaxation phase and is expanded passively by the LV output. The aortic valve is not yet open by that time, and the LV output is not ejected to the aorta. b. When the RV begins to contract later than the LV, the aortic valve opens and blood is ejected into the aorta. c, A fraction of the RV output flows toward the LV, and the LV is paradoxically dilated. B. Spontaneous cardiac rhythm. Well-coordinated contraction of the 2 ventricles results in a simple output pattern without interventricular to-and-fro flow.

Acknowledgment

References

[1] Fontan F, Baudet E. Surgical repair of tricuspid atresia. Thorax 1971;26:240.
[2] Kreutzer G, Galindez E, Bono H, et al. An operation for the correction of tricuspid atresia. J Thorac Cardiovasc Surg 1973;66:613.
[3] Choussat A, Fontan F, Bosso P, et al. Selection criteria for Fontan's procedure. In: Anderson RH, Shinebourne EA, editors. Paedia Cardiol. Edinburgh: Churchill Livingstone; 1977. p. 559–66.
[4] Marcelletti C, Mazzera E, Olthof H, et al. Fontan's operation: an expanded horizon. J Thorac Cardiovasc Surg 1980;80:764–9.
[5] Russo P, Danielson DK, Puga FJ, et al. Modified Fontan procedure for biventricular hearts with complex forms of double-outlet right ventricle. Circulation 1988;78 (Suppl 3):20–5.
[6] Yamamura H, Nakazawa M, Park I, et al. Asynchronous volume change of the two ventricles after Fontan operation in patients with a biventricular heart. Heart Vessels 1994;9:307–14.
[7] Sutton MG, Plappert T, Hilpisch KE, et al. Sustained reverse left ventricular structural remodeling with cardiac resynchronization at one year is a function of etiology: Quantitative Doppler echocardiographic evidence from the Multicenter InSync Randomized Clinical Evaluation (MIRACLE). Circulation 2006;113:266–72.
[8] Tanabe M, Dohi K, Onishi K, et al. Biventricular pacing worsened dyssynchrony in heart failure patient with right-bundle branch block. Int J Cardiol 2010;138: e47–50.
[9] Chalil S, Foley PW, Khadjooi K, et al. Effects of cardiac resynchronization therapy in patients unselected for mechanical dyssynchrony. Int J Cardiol Feb 24 2009 [Electronic publication ahead of print].
[10] Coats AJ. Ethical authorship and publishing. Int J Cardiol 2009;131:149–50.

Contents lists available at ScienceDirect

Journal of Molecular and Cellular Cardiology

journal homepage: www.elsevier.com/locate/yjmcc

Original article

Inositol 1,4,5-trisphosphate receptors are essential for the development of the second heart field

Maki Nakazawa [a,1], Keiko Uchida [a,1], Megumi Aramaki [a], Kazuki Kodo [a], Chihiro Yamagishi [a], Takao Takahashi [a], Katsuhiko Mikoshiba [b,c], Hiroyuki Yamagishi [a,*]

[a] Department of Pediatrics, Keio University School of Medicine, 35 Shinanomachi, Shinjuku-ku, Tokyo 160-8582, Japan
[b] Calcium Oscillation Project, ICORP-SORST, Japan Science and Technology Agency, 2-1, Hirosawa, Wako, Saitama 351-0198, Japan
[c] Laboratory for Developmental Neurobiology, Brain Science Institute (BSI), RIKEN, 2-1 Hirosawa, Wako, Saitama 351-0198, Japan

ARTICLE INFO

ABSTRACT

Congenital heart defects (CHDs) occur in 0.5–1% of live births, yet the underlying genetic etiology remains mostly unknown. Recently, a new source of myocardial cells, namely the second heart field (SHF), was discovered in the splanchnic mesoderm. Abnormal development of the SHF leads to a spectrum of outflow tract defects, such as persistent truncus arteriosus and tetralogy of Fallot. Intracellular Ca^{2+} signaling is known to be essential for many aspects of heart biology including heart development, but its role in the SHF is uncertain. Here, we analyzed mice deficient for genes encoding inositol 1,4,5-trisphosphate receptors (IP$_3$Rs), which are intracellular Ca^{2+} release channels on the endo/sarcoplasmic reticulum that mediate Ca^{2+} mobilization. Mouse embryos that are double mutant for IP$_3$R type 1 and type 3 (IP$_3$R1$^{-/-}$IP$_3$R3$^{-/-}$) show hypoplasia of the outflow tract and the right ventricle, reduced expression of specific molecular markers and enhanced apoptosis of mesodermal cells in the SHF. Gene expression analyses suggest that IP$_3$R-mediated Ca^{2+} signaling may involve, at least in part, the Mef2C–Smyd1 pathway, a transcriptional cascade essential for the SHF. These data reveal that IP$_3$R type 1 and type 3 may play a redundant role in the development of the SHF.

© 2011 Elsevier Ltd. All rights reserved.

1. Introduction

Heart development occurs through the precise orchestration of many anatomical events [1,2]. Soon after gastrulation, mesodermal progenitor cells within an anterior region of the embryo are fated to the cardiac lineage in a bilaterally symmetric fashion. This region is referred to as the cardiac crescent, or the first heart field, and gives rise to a linear beating tube. Recently, it has been revealed that there is a second source of myocardial cells lying medially to the crescent, termed the second heart field (SHF) [3]. As the heart tube forms, cells derived from the SHF, expressing the LIM-homeodomain transcription factor, Islet1 (Isl1) [4], localize in the pharyngeal mesoderm dorsal to the heart tube. Deployment of cells from the SHF to the anterior pole of the heart tube results in the extension of the outflow

tract, which is essential for proper alignment of the base of the great arteries with the ventricles during cardiac development [5].

Ca^{2+} signaling is essential for many aspects of cardiac function [6]. In the mature cardiomyocyte, Ca^{2+} influxes into the cytoplasm and Ca^{2+} release from the sarcoplasmic reticulum, allows actin–myosin interactions and contraction [7]. Intracellular Ca^{2+} signaling cascades also play an important role in cardiomyocyte hypertrophy [6], and may regulate cardiac gene expression during development. Mouse embryos cultured at embryonic day (E) 7.5–8.5 in the presence of the L-type Ca^{2+} channel blockers develop defective hearts [8], suggesting that the proper influx of Ca^{2+} for intracellular Ca^{2+} signaling is essential for the early morphogenesis of the heart.

Inositol 1,4,5-trisphosphate receptors (IP$_3$Rs) are intracellular Ca^{2+} release channels that mediate Ca^{2+} mobilization from the endo/ sarcoplasmic reticulum to the cytoplasm in response to the binding of inositol 1,4,5-trisphosphate (IP$_3$) [9]. The Ca^{2+} release induced by IP$_3$ is triggered by various external stimuli and plays important physiological roles in various cell types and tissues. Three IP$_3$R subtypes have been identified in mammals. IP$_3$R type 1 (IP$_3$R1) plays critical roles in the regulation of motor and learning systems [10], whereas IP$_3$R type 2 and type 3 (IP$_3$R2 and IP$_3$R3) have a redundant role in exocrine physiology underlying energy metabolism [11]. Recently, we reported a redundant role of IP$_3$R1 and IP$_3$R2 during cardiogenesis, implicating the calcineurin/NFAT signaling pathway in the development of heart valves and

    * Corresponding author. Tel.: +81 3 5363 3515; fax: +81 3 5379 1978.
    E-mail address: hyamag@sc.itc.keio.ac.jp (H. Yamagishi).
    [1] Contributed equally to this work.

Table 1
Genotypes of embryos from $IP_3R1^{+/-}3^{-/-}$ intercrosses.

| Genotype | IP$_3$R1 | +/+ | +/− | −/− | Total |
	IP$_3$R3	−/−	−/−	−/−	
E8.5	Observed	31	54	19	104
	Expected	26	52	26	
E9.5	Observed	79	168	68	315
	Expected	79	158	79	
E10.5	Observed	7	7	6	20
	Expected	5	10	5	
E11.5	Observed	13	10	5	28
	Expected	7	14	7	
E12.5	Observed	7	12	0	19
	Expected	5	10	5	

muscle [12]. Here, we show that IP$_3$R1 and IP$_3$R3 are redundantly essential for heart development, especially for the SHF, and we propose a model in which IP$_3$Rs mediate intracellular Ca^{2+} signaling to regulate a cardiogenic transcriptional cascade.

2. Materials and methods

2.1. Mouse genetic studies

Mice heterozygous null or homozygous null for IP$_3$R1 or IP$_3$R3 have been previously described [10,11]. $IP_3R1^{+/-}IP_3R3^{-/-}$ mice were intercrossed to generate embryos that are homozygous null for both IP$_3$R1 and IP$_3$R3 ($IP_3R1^{-/-}IP_3R3^{-/-}$). Genomic DNA samples prepared from tail biopsies or yolk sacs were subjected to PCR genotyping analysis as described previously [10,11].

2.2. Whole-mount in situ hybridization

Whole-mount in situ hybridizations were performed using digoxigenin-labeled antisense riboprobes as described previously [13].

2.3. Section in situ hybridizations

Section in situ hybridizations were performed using digoxigenin-labeled antisense riboprobes synthesized from a 588 bp fragment of mouse Isl1 cDNA and a 527 bp fragment of mouse Bmp4 cDNA (Genostaff Co., Ltd.) as reported previously [14].

2.4. Cell proliferation assay and TUNEL analysis

Cell proliferation assays were performed on paraffin sections by immunohistochemistry with anti-phospho-histone H3 (Ser10) antibody (Upstate) and AlexaFluor488 conjugated anti-rabbit IgG for fluorescence microscopy. TUNEL analysis was performed on paraffin
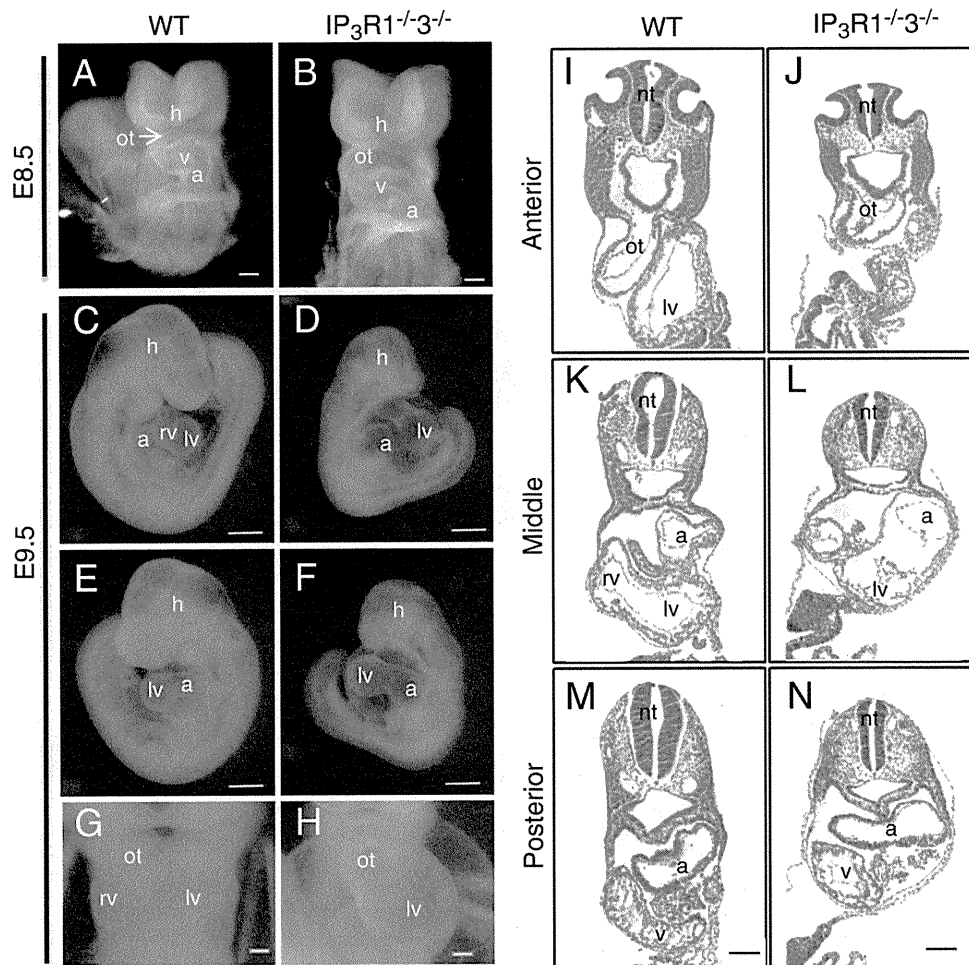

Fig. 1. Cardiac defects in $IP_3R1^{-/-}3^{-/-}$ embryos. Mouse embryos at E8.5 (A and B) and E9.5 (C–H) for wildtype (A, C, E and G) and $IP_3R1^{-/-}3^{-/-}$ (B, D, F and H) are shown in the frontal (A and B), right lateral (C and D), left lateral (E and F) views, and frontal views focusing on the heart (G and H). Hematoxylin and eosin-stained transverse sections of the anterior (I and J), middle (K and L) and posterior (M and N) segments of the hearts of wildtype (I, K and M) and $IP_3R1^{-/-}3^{-/-}$ (J, L and N) embryos at E9.5 are shown. $IP_3R1^{-/-}3^{-/-}$ embryos initiated rightward looping at E8.5 (B), but had a shortened outflow tract and no obvious right ventricular segment at E9.5 (D, H, J and L). a, atria; h, head; lv, left ventricle; nt, neural tube; ot, outflow tract; v, ventricle. Scale bars, 0.1 mm (A, B, G, H and I–N); 0.5 mm (C–F).

sections using an apoptosis detection kit (ApopTag, Intergen) following the manufacturer's protocol.

2.5. Microarray analysis and qRT-PCR

Total RNA was extracted from the E9.25 heart of $IP_3R1^{-/-}IP_3R3^{-/-}$ or $IP_3R1^{+/-}IP_3R3^{-/-}$ embryo using RNeasy (QIAgen) and was amplified using the WT-Ovation Pico RNA Amplification System (NuGEN) to obtain biotinylated cDNA. Biotinylated cDNA from one heart of each embryo was applied to a microarray analysis using the Affymetrix Genechip (Mouse 430.2) (n = 2). Arrays were subjected to Robust Multichip Average (RMA) analysis. The fold change was calculated and Student's t-test was performed to determine statistically significant differences. For quantitative RT-PCR analysis of Smyd1 and Mef2c expression, cDNA was synthesized using the High Capacity cDNA Archive

kit (Applied Biosystems) from the total RNA extracted from E9.25 heart of $IP_3R1^{-/-}IP_3R3^{-/-}$ or $IP_3R1^{+/-}IP_3R3^{-/-}$ embryo. The cDNA was used as a template in a TaqMan Real-Time PCR with the ABI 7500 Real-Time PCR system (Applied Biosystems). The data are normalized to the levels obtained for GAPDH. The TaqMan probes used for Smyd1, Mef2c and GAPDH were Mm00477663_m1, Mm01340842_m1 and Mm99999915_g1 (Applied Biosystems), respectively.

3. Results

3.1. Redundant roles of IP₃R1 and IP₃R3 in cardiac development

To determine whether IP₃Rs play a role in cardiac development, we set out to delineate the cardiac phenotype of IP₃R mutant mouse embryos. Because single IP₃R knockout mice and $IP_3R2^{-/-}IP_3R3^{-/-}$ mice are
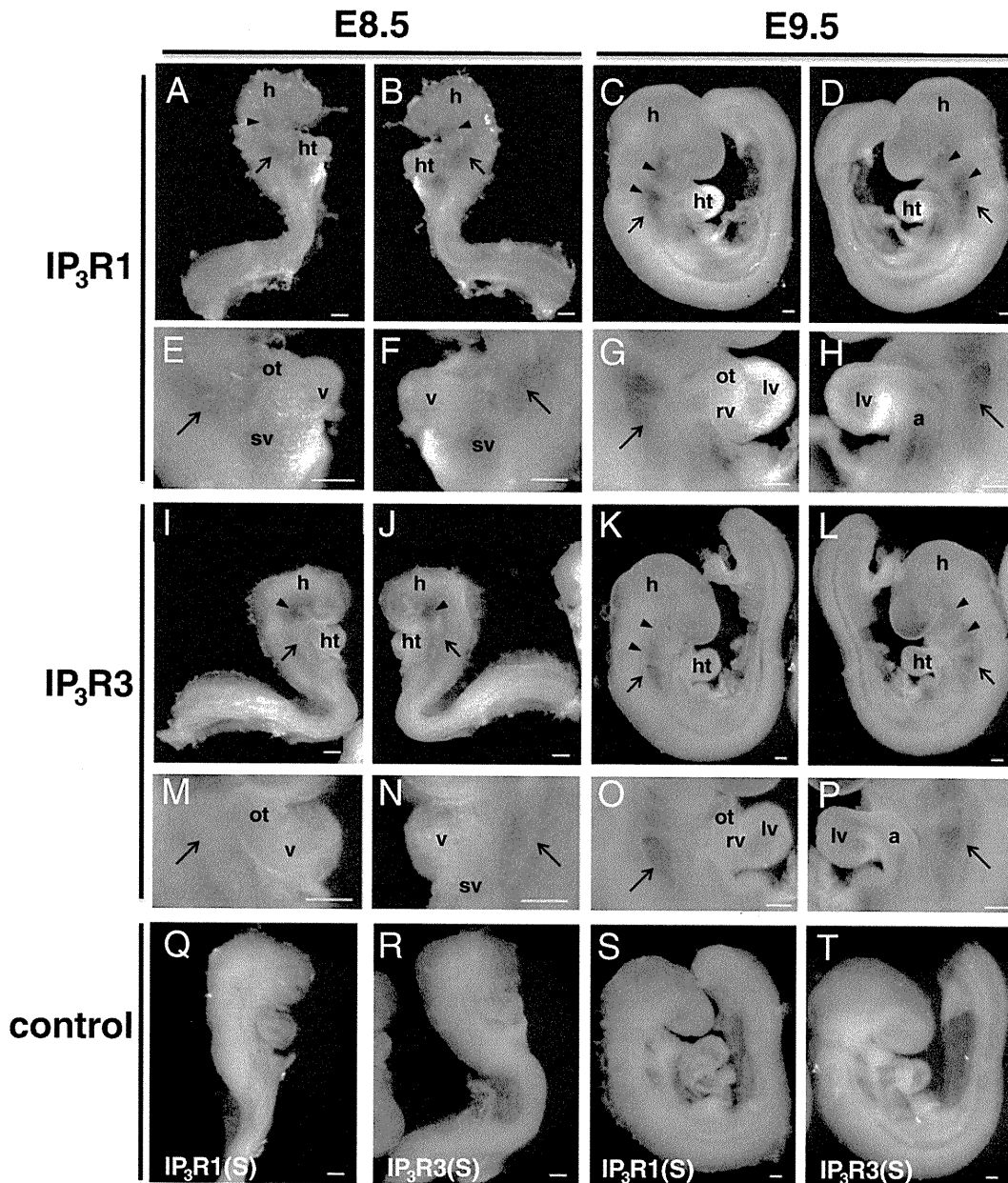

Fig. 2. Both IP₃R1 and IP₃R3 are expressed in the SHF. Expression of IP₃R1 (A–H) and IP₃R3 (I–P) were examined in wildtype embryos at E8.5 and E9.5 by whole-mount in situ hybridization. Whole-mount views (A–D and I–L) and close-up views of the hearts (E–H and M–P) are shown. Control data using sense probes are shown (Q–T). IP₃R1 began to be expressed in the first and second pharyngeal arches (arrowheads), the outflow tract, the pharyngeal/splanchnic mesoderm, or the SHF (arrows), and the sinus venosus at E8.5 (A, B, E and F), and expanded to the right ventricle and the atria at E9.5 (C, D, G and H). IP₃R3 began to be expressed in the first and second pharyngeal arches (arrowheads), the outflow tract, and the SHF (arrows) at E8.5 (I, J, M and N) similarly to the expression of IP₃R1, and expanded to the right ventricle at E9.5 (K, L, O and P).

normally born with no cardiac phenotype [10,11], we generated embryos homozygous null for both IP_3R1 and IP_3R3 ($IP_3R1^{-/-}IP_3R3^{-/-}$) by intercrossing phenotypically normal and fertile $IP_3R1^{+/-}IP_3R3^{-/-}$ mice.

As summarized in Table 1, no $IP_3R1^{-/-}IP_3R3^{-/-}$ embryos were observed at E12.5, whereas the expected Mendelian distribution of genotypes was observed before E10.5. All $IP_3R1^{-/-}IP_3R3^{-/-}$ embryos collected between
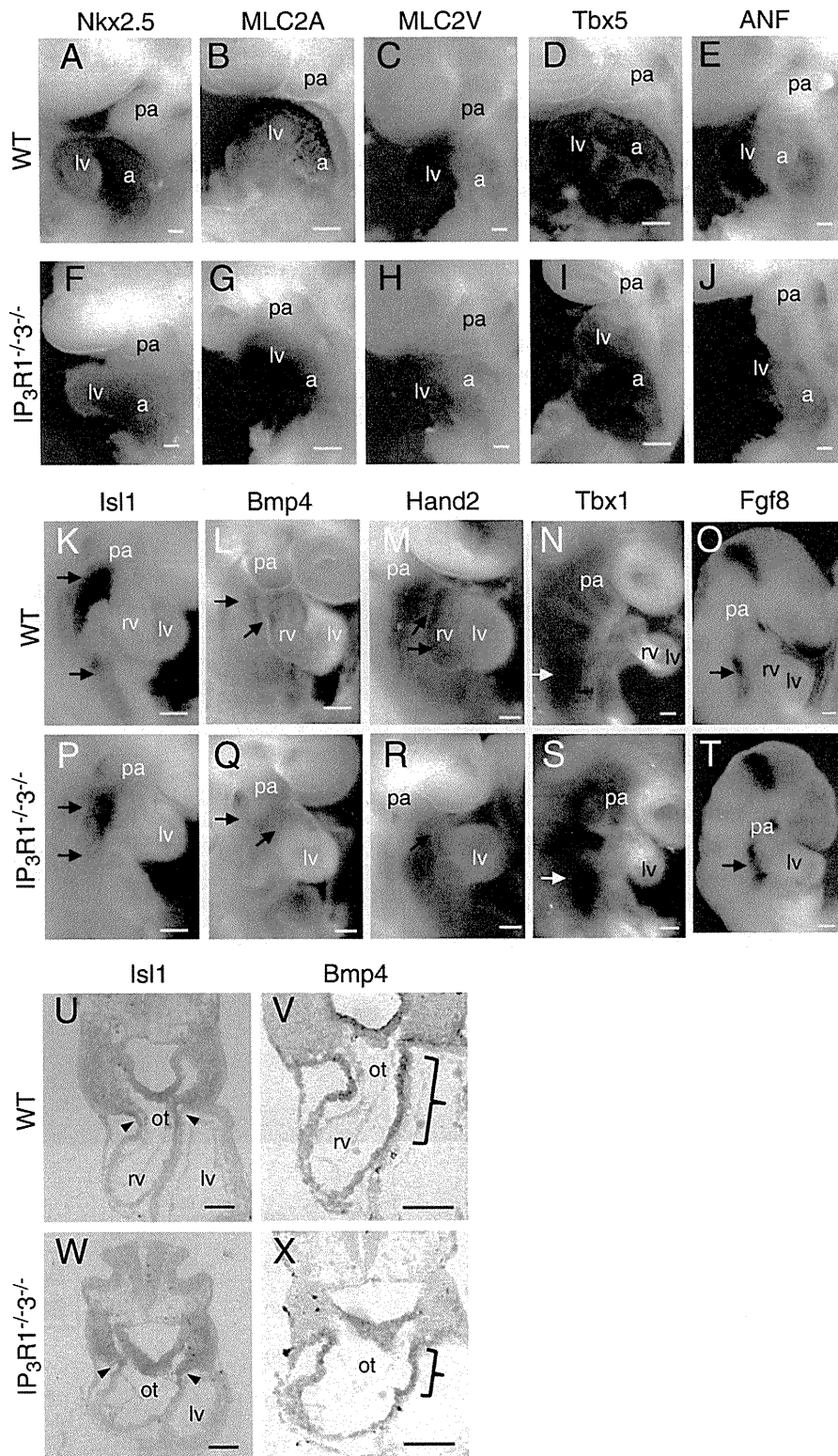

Fig. 3. Expression of cardiac development markers in $IP_3R1^{-/-}3^{-/-}$ embryos. Whole-mount (A–T) and section (U–X) *in situ* hybridization of wildtype (A–E, K–O, U and V) and $IP_3R1^{-/-}3^{-/-}$ (F–J, P–T, W and X) embryos at E9.25 are shown. *Nkx2.5, MLC2A, MLC2V, Tbx5,* and *ANF* are expressed at a normal level in $IP_3R1^{-/-}3^{-/-}$ embryos compared to wildtype (A–J). *Isl1* expression in the pharyngeal splanchnic mesoderm adjacent to the outflow tract (arrows in K and P and arrowheads in U and W) is reduced in $IP_3R1^{-/-}3^{-/-}$ embryos (P,W) compared to wildtype (K,U). *Bmp4*-expressing cells were detectable, but the expressing region was restricted in $IP_3R1^{-/-}3^{-/-}$ embryos compared with wildtype (arrows in L and Q and rectangle in V and X). Also, *Hand2* expressing cells were detectable, but the expressing region was restricted in $IP_3R1^{-/-}IP_3R3^{-/-}$ embryos (arrow in R) compared to wildtype (arrows in M). *Tbx1* and *Fgf8* are expressed in the SHF of $IP_3R1^{-/-}3^{-/-}$ embryos (arrow in S and T) similar to wildtype (arrow in N and O). pa, pharyngeal arch; ot, outflow tract; rv, right ventricle; lv, left ventricle. Scale bars, 0.1 mm.

E10.5 and 11.5 presented with marked growth retardation and pericardial effusion, suggesting that the $IP_3R1^{-/-}IP_3R3^{-/-}$ embryos die around E11.5, consistent with their absence at E12.5.

Morphological analysis of the heart development of $IP_3R1^{+/-}IP_3R3^{-/-}$ embryos confirmed that they show normal cardiogenesis. Analysis of $IP_3R1^{-/-}IP_3R3^{-/-}$ embryos at E8.5 showed a normal heart with the S-shaped structure demarcated into the outflow tract region on the right side, the common ventricular region in the middle, and the common atrial region on the left side (Figs. 1A and B) with no sign of growth retardation. $IP_3R1^{-/-}IP_3R3^{-/-}$ embryos at E9.5 begin to present with growth retardation and develop a pericardial effusion. Their hearts showed a shortened outflow tract that appeared to directly connect to a single left ventricle with no obvious right ventricular segment. The hearts of wildtype mice had a distinctive outflow tract, and primitive right and left ventricular segments (Figs. 1C–H). These observations suggest that in $IP_3R1^{-/-}IP_3R3^{-/-}$ mutant mice, heart development is arrested during formation of the outflow tract and the right ventricle while the rightward looping of the heart is initiated. Therefore, we hypothesize that IP₃R1 and IP₃R3 redundantly play an important role in the development of the SHF that gives rise to the outflow tract and the right ventricle.

Because phenotypic analysis of $IP_3R1^{-/-}IP_3R3^{-/-}$ mutant embryos indicated defects in the SHF, we examined the expression patterns of IP₃R1 and IP₃R3 by in situ hybridization, focusing on the development of the SHF. At E8.5, IP₃R1 is expressed in the outflow tract and the dorsal area of the primitive heart tube, including the pharyngeal splanchnic mesoderm, the SHF, and the sinus venosus (Figs. 2A, B, E and F). By E9.5, the expression of IP₃R1 expanded from the outflow tract to the right ventricle and the atria (Figs. 2C, D, G and H). IP₃R3 is also expressed in the SHF in the pharyngeal region and the outflow tract of the primitive heart from E8.5 (Figs. 2I, J, M and N), and later expanded to the right ventricle at E9.5 (Figs. 2K, L, O and P). Overlapping expression of IP₃R1 and IP₃R3 in the SHF at E8.5–9.5 is consistent with the cardiac phenotype of $IP_3R1^{-/-}IP_3R3^{-/-}$ mutant embryos.

3.2. Developmental defects of the SHF in $IP_3R1^{-/-}IP_3R3^{-/-}$ mutant embryos

In order to identify and analyze the chamber differentiation of $IP_3R1^{-/-}IP_3R3^{-/-}$ hearts, we performed a series of whole-mount in situ hybridizations using molecular markers. The earliest markers for
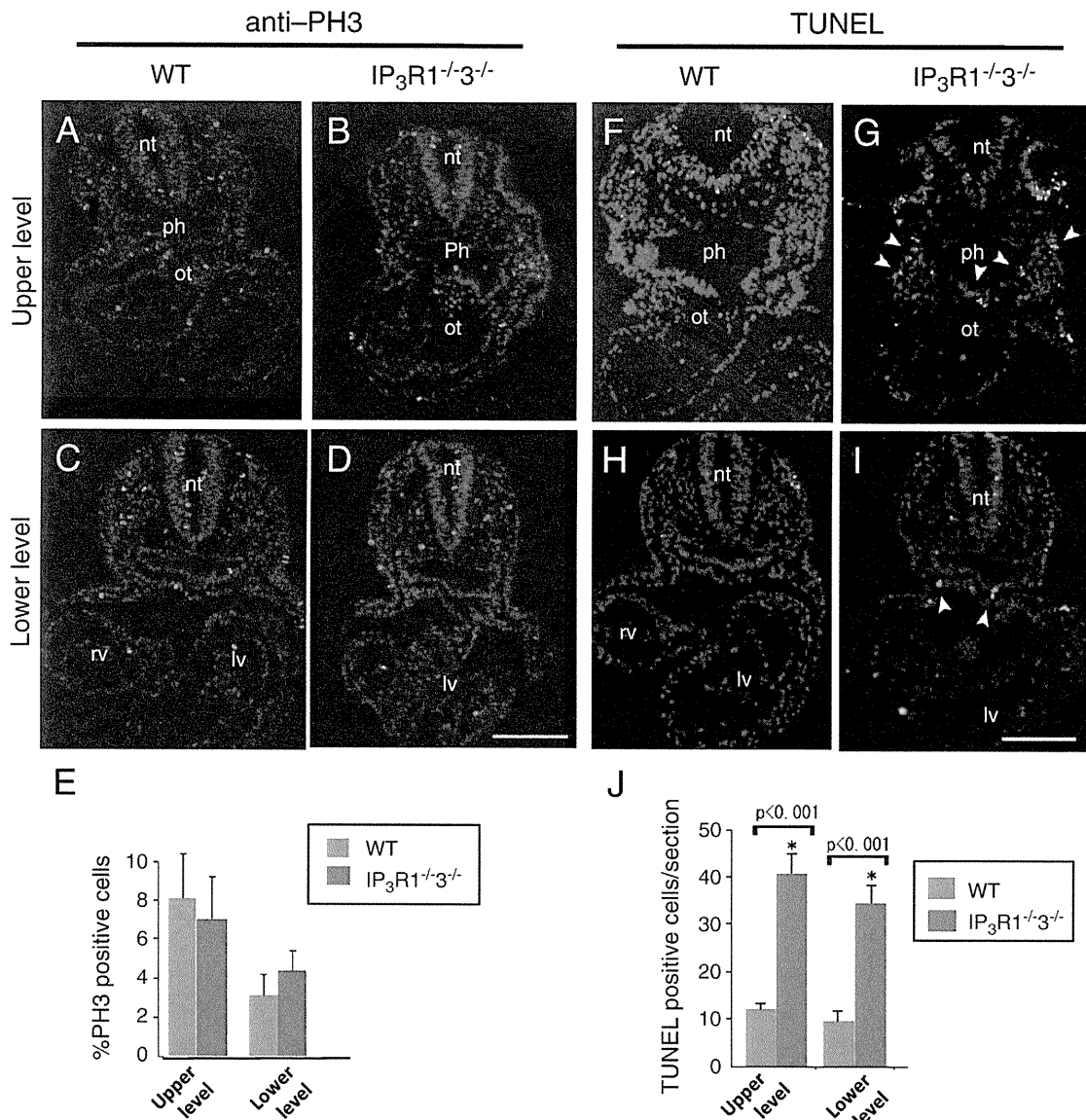

Fig. 4. Enhanced apoptosis in the SHF of $IP_3R1^{-/-}3^{-/-}$ embryos. Transverse sections at E9.0 were analyzed using anti-phospho-histone H3 (PH3) antibody (A–E) and by TUNEL assay (F–J) in wildtype (A, C, F and H) and $IP_3R1^{-/-}3^{-/-}$ embryos (B, D, G and I). Sections were counterstained with DAPI, and the green signals indicate the nuclei of the PH3-positive cells (A–D) and TUNEL-positive cells (F–I). Cell proliferation appears relatively normal (A–E), but apoptotic signals are significantly enhanced (J) in the probable pharyngeal splanchnic mesoderm in $IP_3R1^{-/-}3^{-/-}$ embryos (arrowheads in G and I) compared with wildtype (F and H). lv, left ventricle; nt, neural tube; ot, outflow tract; ph, pharynx; rv, right ventricle. Scale bars, 0.1 mm.

cardiomyocyte differentiation, Nkx2.5 and myosin light chain (Mlc) 2a [15,16], and the earliest marker for ventricular differentiation, Mlc2v, are expressed in the hearts of $IP_3R1^{-/-}IP_3R3^{-/-}$ mutants as well as wildtype mice at E9.25 (Figs. 3A–C and F–H). Tbx5 and the atrial natriuretic factor gene (ANF) are predominantly expressed in the left ventricle [17] and are expressed in $IP_3R1^{-/-}IP_3R3^{-/-}$ mutants as well as wildtype mice (Figs. 3D, E, I and J). These data indicate that normal cardiomyocyte differentiation occurred, but the development of the right ventricle and the outflow tract is defective in $IP_3R1^{-/-}IP_3R3^{-/-}$ embryos.

To elucidate the mechanism underlying the developmental defect in $IP_3R1^{-/-}IP_3R3^{-/-}$ embryos, we analyzed the expression levels of genes essential for the SHF in embryos at E9.25. Isl1 is the earliest marker of the SHF and is expressed throughout the pharyngeal region [4] (Fig. 3K). In $IP_3R1^{-/-}IP_3R3^{-/-}$ embryos, the expression area of Isl1 is markedly reduced in the pharyngeal splanchnic mesoderm (Fig. 3P). In situ hybridization of tissue sections shows Isl1 expression in the pharyngeal mesoderm adjacent to the outflow tract in both wildtype and $IP_3R1^{-/-}IP_3R3^{-/-}$ mutant embryos, however, Isl1-expressing pharyngeal mesoderm is hypoplastic in $IP_3R1^{-/-}IP_3R3^{-/-}$ embryos compared to wildtype embryos (Figs. 3U and W). Bone morphogenetic protein (Bmp) signal transduction is necessary in the SHF [18] with Bmp4 being expressed in the first pharyngeal arch, splanchnic mesoderm, outflow tract, and right ventricle in wildtype embryos [19] (Fig. 3L). In $IP_3R1^{-/-}IP_3R3^{-/-}$ embryos, the expression of Bmp4 is reduced in the splanchnic mesoderm and the heart compared to wildtype, while it is unaffected in the first pharyngeal arch (Fig. 3Q). In situ hybridization detected Bmp4-expressing cells in a relatively restricted region of the outflow tract in $IP_3R1^{-/-}IP_3R3^{-/-}$ embryos compared to wildtype embryos. This reflected a shortened outflow tract and a hypoplastic right ventricle in $IP_3R1^{-/-}IP_3R3^{-/-}$ mutants (Figs. 3V and X). A gene encoding the basic helix–loop–helix transcription factor, Hand2, is predominantly expressed in the outflow tract and the right ventricle as well as in the pharyngeal mesenchyme in wildtype embryos [20] (Fig. 3M). Consistent with the patterns of Isl1 and Bmp4 expression, the expression of Hand2 is markedly downregulated in the outflow tract region of the heart in $IP_3R1^{-/-}IP_3R3^{-/-}$ mutant embryos (Fig. 3R). This further demonstrates hypoplasia of the outflow tract and the right ventricle that is derived from the SHF.

In contrast to Isl1, Bmp4 and Hand2, the expression of a T-box transcription factor, Tbx1, and a fibroblast growth factor, Fgf8, is not affected in $IP_3R1^{-/-}IP_3R3^{-/-}$ mutant embryos (Figs. 3S and T) at E9.25 compared to wildtype embryos (Figs. 3N and O). Tbx1 is normally expressed in the mesoderm and endoderm of pharyngeal arches including the SHF, and is required for the maintenance of Fgf8 expression in the SHF at E9.0–9.5 [21]. These observations suggest a specific defect of the SHF in $IP_3R1^{-/-}IP_3R3^{-/-}$ mutants rather than global defects.

To determine whether hypoplasia of the outflow tract and the right ventricle in $IP_3R1^{-/-}IP_3R3^{-/-}$ hearts results from impaired cell proliferation or enhanced apoptosis of the SHF, we performed immunohistochemistry of the cell proliferation marker, phosphohistone H3 (PH3), and TUNEL assays for apoptosis in $IP_3R1^{-/-}IP_3R3^{-/-}$ embryos at E9.0, just prior to the stage when morphological abnormalities become apparent. Cell proliferation was observed at near normal levels in $IP_3R1^{-/-}IP_3R3^{-/-}$ embryos as determined by immunohistochemistry using anti-PH3 (Figs. 4A–E). In contrast, a number of apoptotic cells were detectable in the probable pharyngeal mesoderm where overlapped with the Isl1-expressing region [4] in $IP_3R1^{-/-}IP_3R3^{-/-}$ embryos that showed a statistically significant increase compared to wildtype littermates (Figs. 4F–J). These results suggest that IP3R1 and IP3R3 are redundantly essential for the survival of cells in the SHF.

3.3. Analysis of gene expression that is dependent on IP₃R-mediated Ca^{2+} signaling during heart development

To investigate the molecular mechanisms underlying the defect in heart development in $IP_3R1^{-/-}IP_3R3^{-/-}$ mice, we compared gene expression profiles between the mutant and wildtype hearts at E9.25 using microarray analysis. Several genes related to cardiac development were significantly downregulated in mutant hearts, including phospholamban, calsequestrin2 and Nfatc, which are involved in Ca^{2+} signaling (Table 2). Intriguingly, the expression of the Smyd1 gene, which encodes a transcriptional repressor and putative histone methyltransferase, is decreased 0.636 fold, and that of a MADS-box transcription factor, Mef2c, is decreased 0.835 fold (Table 2). Smyd1 is a regulator of right ventricular heart development and the SHF. The Smyd1 gene is a direct transcriptional target of Mef2c in the developing heart [22]. Our qRT-PCR data confirmed the downregulation of both Smyd1 and Mef2c expression in $IP_3R1^{-/-}IP_3R3^{-/-}$ hearts (Figs. 5A and B). Our whole-mount in situ hybridization analysis showed downregulation of Smyd1 in $IP_3R1^{-/-}IP_3R3^{-/-}$ hearts consistent with the microarray and qRT-PCR data (Fig. 5C).

Table 2
Gene microarray data from the $IP_3R1^{-/-}3^{-/-}$ versus $IP_3R1^{-/-}3^{+/-}$ heart at E9.25.

Gene symbol	Gene function	Accession no.	Fold change	p value
Pln	Phospholamban	Mm.34145	0.390	0.0093703
Casq2	Calsequestrin 2	Mm.15343	0.481	0.027505
Nfatc1	Nuclear factor of activated T-cells, cytoplasmic, calcineurin-dependent 1	Mm.329560	0.521	0.0097186
Atp1a2	ATPase, Na+/K+ transporting, alpha 2 polypeptide	Mm.207432	0.633	0.014535
Smyd1 (Bop)	SET and MYND domain containing 1	Mm.234274	0.636	0.0063516
Fbn1	Fibrillin 1	Mm.271644	0.645	0.0116202
Zfp697	Zinc finger protein 697	Mm.442892	0.661	0.0257862
Adam19	A disintegrin and metallopeptidase domain 19 (meltrin beta)	Mm.89940	0.661	0.0291554
Casp8	Caspase 8	Mm.336851	0.662	0.0202887
Hif1a	Hypoxia inducible factor 1, alpha subunit	Mm.3879	0.687	0.0084657
Hbegf	Heparin-binding EGF-like growth factor	Mm.289681	0.696	0.0011363
Txnrd2	Thioredoxin reductase 2	Mm.390906	0.725	0.018006
Irx4	Iroquois related homeobox 4 (Drosophila)	Mm.103784	0.732	0.0117921
Casp7	Caspase 7	Mm.35687	0.737	0.0049145
Atp2a2	ATPase, Ca++ transporting, cardiac muscle, slow twitch 2	Mm.227583	0.818	0.0151468
Nfatc3	Nuclear factor of activated T-cells, cytoplasmic, calcineurin-dependent 3	Mm.383185	0.826	0.0387645
Pten	Phosphatase and tensin homolog	Mm.245395	0.826	0.0221523
Ednra	Endothelin receptor type A	Mm.283168	0.831	0.0472732
Mef2c	Myocyte enhancer factor 2C	Mm.436781	0.835	0.0459879
Myh6	Myosin, heavy polypeptide 6, cardiac muscle, alpha	Mm.290003	0.856	0.0025503
Tnnt2	Troponin T2, cardiac	Mm.247470	0.868	0.0320203
Ppp3cb	Protein phosphatase 3, catalytic subunit, beta isoform	Mm.274432	0.880	0.0407585

Fold change is a ratio of expression level compared with wildtype set to 1.0.